A review on Nanocomposites
Part 1: Mechanical Properties

Bao Le, first author
Mechanical and Construction Engineering Department
Northumbria University
Newcastle upon Tyne NE1 8ST, UK
bao.le@northumbria.ac.uk

Jibran Khaliq, second author
Mechanical and Construction Engineering Department
Northumbria University
Newcastle upon Tyne NE1 8ST, UK
jibran.khaliq@northumbria.ac.uk

Dehong Huo, third author
Mechanical Engineering, School of Engineering
Newcastle University
Newcastle upon Tyne NE1 7RU
dehong.huo@newcastle.ac.uk

Xiangyu Teng, fourth author
Mechanical Engineering, School of Engineering,
Newcastle University
Newcastle upon Tyne NE1 7RU
txy19910914@hotmail.com

Islam Shyha, fifth author[1]
Mechanical and Construction Engineering Department
Northumbria University
Newcastle upon Tyne NE1 8ST, UK
islam.shyha@northumbria.ac.uk

---

[1] Corresponding author

ABSTRACT

Micromachining of nanocomposites is deemed to be a complicated process due to the anisotropic, heterogeneous structure and advanced mechanical properties of these materials associated with the size effects in micromachining. It leads to poorer machinability in terms of high cutting force, low surface quality and high rate of tool wear. In part 1 of this two-part review paper, a comprehensive review on mechanical properties of various nanocomposites will be presented while the second part of the paper will focus on the micro-machinability of these nanocomposite materials.

***Keywords**: nanocomposites; micromachining; manufacturing; materials; mechanical properties*

1. INTRODUCTION

The word ”nanocomposite” was first introduced by Blumstein in 1961 [1]. The primitive nanocomposite was investigated in an attempt to improve the thermal stability of nano-silicate reinforced polymethyl methacrylate (PMMA) [2] in 1965. Nanocomposites share similar terminologies as conventional composites in terms of their constituents except for the reinforcement size that is typically in the range of hundreds of nanometers. The reduction from micro-range to nano-range of fillers provides remarkable reinforcements in nanocomposites while requiring much lower content of fillers than the composites with conventional sizes(hereafter, call composites or conventional composites for short), hence leading to inconsiderable increases in weight [3]. Nowadays, many nanocomposites have been discovered and commercially applied in various industrial areas including (and not limited to) aerospace [4], automobile [5] and medicine [6] due to their superior properties, namely mechanical [7], thermal [8], electrical [9], electrochemical, electromagnetic [10], and gas barrier properties [11]. Due to these superior properties, further applications of nanocomposites have been found in terms of manufacturing micro-structured components following the miniaturization trend of modern production. The discovery of nanocomposites has found many applications in microelectronics (Figure 1a, b) [12]. Tang et al. [13] have concluded that carbon nanotubes (CNTs) reinforced polyimide nanocomposite is applicable for microelectronics devices due to its ideal electrical conductivity, storage modulus and environmental stability. Other applications such as high performance transistors from poly-4-vinylphenol (PVP)/ TiO2 nanocomposite [14] or high energy density capacitor from poly-vinylidene-fluoride/TiO2 nanocomposite [15] have exhibited better operations than their neat matrix counterparts. Moreover, this miniaturization trend could cover not only microelectronics but also micromechanical devices. Nanocomposites might be considered as alternatives to composites and alloys in manufacturing micro-products [16]. For example, manufacturing airframe [17] or wings [18] of micro-air vehicles (MAVs) using conventional composites [19] such as carbon fiber, glass fiber or Kevlar reinforced plastics could be replaced by CNTs or carbon nanofiber (CNF) nanocomposites that have higher strength-to-weight ratio and flexibility. The artificial wings for MAVs have been developed using CNT/Epoxy and CNT/PP nanocomposites by Kumar et al. [20]. Additionally, the additions of ceramic nanoparticles improved the tribological property, wear-resistance and overall mechanical properties of metal nanocomposites [21]. Therefore, these nanocomposites could be used in manufacturing pistons or linkage rods [22] (Figure 1c), micro-gears [23] (Figure 1d-f). Due to their huge potentials to produce micro-products, it would be necessary to investigate on the mechanical properties as well as feasible processing methods to fabricate nanocomposites. Most of the recent techniques (Table 1) to manufacture nanocomposites are incapable of producing a final product (in terms of dimensional and geometrical accuracies as well as surface quality), instead, a near-net-shape is produced. Therefore, post-processing or finishing technologies will be always required. Some manufacturing processes such as LIGA (Lithography, Electroplating, and Molding) [24], laser micromachining [25], microextrusion additive manufacturing [26], micro-EDM (Electrical Discharge Machining) [27] , and mechanical micromachining [28] have been used to generate small precision component and micro-structured parts [29].

2. NANOCOMPOSITES

In general, nanocomposites still keep the distinct characteristics of both matrix and fillers that make them different from alloys while their final properties depend on their matrix-filler interface bonding, the arrangement of fillers inside the matrix as well as the geometry and content of the fillers. Nanocomposites are also distinguished from composites in which one of the filler's dimensions is in the range of 1-100 nm**.** Table 2 demonstrates a few fundamental geometries of typical nano-fillers. The specific properties of each category, as well as the effect of filler phases on them, will be discussed in the next sections. Based on the unique properties of different nanocomposites, their potential or commercial applications will be given. In parallel with the discussion about nanocomposites, a comparison between nanocomposites and composites will be addressed to identify the basic differences in terms of the influences of size, content and properties of the filler on their properties.

2.1 Differences between nanocomposites and composites

As mentioned earlier, the basic difference between nanocomposites and traditional composites is the size of fillers. The revolution of composites takes place with the size reduction of the fillers from few millimetres in traditional composites to micro-scale (1-100 µm) in modern composites and recently, nanocomposites with the fillers having dimensions in nano-scale. The original for size reduction of filler is to attain a homogenous distribution of filler within the matrix hence reduce the stress concentrations within the composite structure [30] that subsequently improve its mechanical properties. Furthermore, smaller fillers can obtain higher surface energy that makes stronger bonding with the matrix [31] that is, in turn, improves stiffness and strength of the system [32]. In essence, the reinforcing mechanism of composite could be divided into two main types based on the filler scale. For micro-filler, the continuum mechanism is employed to indicate that the micro-fillers bear a fraction of transferred load from the matrix hence the efficiency of reinforcement depends on the adhesion of matrix-filler interface [33]. For nano-filler (10-100 nm), the strengthening mechanism is applied when the matrix-filler interaction is in the molecular level. This mechanism proclaims that the nano-fillers restrict the plastic deformation of the matrix by impeding its dislocations, subsequently leads to the improvement of strength and hardness.

Some researchers have investigated the influence of filler size on the mechanical properties of polymer composites. It was observed that in micro-range of fillers, their size effect on the tensile modulus of composites was unobvious. Some experimental results indicated that the moduli of epoxy-based composites were not considerably improved, or even decreased [34] while using various particle size of Al_2O_3 (1-12 µm) [35], glass (4.5-62 µm) [36], or silica (2-47 µm) [37]. The same trend could be seen with PP/ $CaCO_3$ [38], poly-benzoxazine/$CaCO_3$ [39] or polyester/ Al [40] (Figure 2). In addition, the relation between the filler size and tensile strength of composite also not clear. While some studies reported that tensile strengths of composites remarkably increased with the size reduction of fillers, using micro silica particles to reinforce epoxy [37, 41], another result showed no trend of tensile strength variation of epoxy/Al_2O_3 when decreasing the filler size [35]. In general, it could be seen that the influence of filler size in micro-scale on mechanical properties of composite is unremarkable.

From the discussion above, it leads to the requirement to investigate the effect of filler size in nano-scales to identify whether their influence on mechanical properties of composites are more sensitive than the micro-counterparts or not. Onuegbu and Igwe [42] adapted various filler sizes (150, 300 and 420 nm) of snail shell powder to reinforce PP. Tensile modulus, flexural strength and impact strength were observed to be improved with the decrease of filler size. However, those improvements were not considerable. For example, the tensile strengths increased by around 5% when decreasing the filler size from 300 to 150 nm for every weight fraction. The improvement of the mechanical properties of composites was only considerable when keep reducing the size of filler below 100 nm. This phenomenon was verified when a comparative study between micro and nano-fillers in terms of mechanical performance of polymer composites was given by Devaprakasam et al. [43]. In this research, micro-silica (100 nm – 4 µm) and nano-silica (40 – 60 nm) were employed and the results exhibited a less variation in the modulus and hardness of the nanocomposite than the composite while applying different loadings. It was explained by the homogenous distribution of nano-fillers, strong interfacial matrix-filler bonding in comparison with micro-fillers. Some other researches also indicated the dominant effect of filler sizes on mechanical properties when they were reduced below 20 nm, as seen in Figure 3. This dominance was also verified by Edwards [44] that a high degree of reinforcement could be achieved using the fillers with sizes in below 100 nm.

This threshold of filler size in which the mechanical properties of composites increase remarkably is called 'critical size', according to [45]. Kumar et al. [46] investigated the effect of CNTs ratio on strengthening behavior of polyethene-based nanocomposites. They claimed that employing high-aspect-ratio CNTs provided great hardness and elastic modulus improvement due to high contact surface area and strong interfacial bonding of CNT-polymer. In addition, the presence of mechanical locking was more frequent in terms of high-aspect-ratio CNT due to its smaller diameter and longer length (Figure 4). However, most of the relevant studies only focused on experimental works while a few theoretical models or simulations were found (Figure 5). Constitutive models would be essential to provide quantitative analysis and explanation in terms of strengthening mechanism. Chowdhury and Okabe [47] have applied molecular dynamic (MD) method to investigate the effect of matrix density, chemical cross-links on the interface and geometrical defect of CNTs on interfacial shear strength (ISS) and consequently, CNT pull-out (Figure 5a). From the simulation, it was concluded that high matrix density, presence of cross-link and small cross-link switching contributed to high ISS. A 3D representative volume element (RVE) method has also been applied to assess the effects of CNT waviness, diameter, volume fraction, Poisson's ratio and matrix modulus on interfacial strength of polymer/SWCNT [48] (Figure 5b). Based on the aforementioned studies, it could be observed that investigating the interfacial bonding between nano-fiber and matrix plays a critical role in load transfer assessment and consequently, the mechanical strengthening efficiency of the reinforcement. The stress transfer behavior of SWCNT in epoxy matrix has been studied by Xiao and Zhang [49] using the Cox model for solid fibers [50] (Figure 5c). The main used indicator was stress transfer efficiency δ which is the ratio of maximum tensile stress (σ_{max}) to maximum shear stress (τ_{max}) in the interfacial section. The effect of SWCNT length, diameter and thickness are shown in Figure 6a. Moreover, a comparison of stress transfer efficiency δ between SWCNT and carbon fiber (CF) has also been expressed with the assumption of the same hollow structure and dimension of CF as SWCNT. The analytical results showed a remarkable improvement of δ (128%) in case of epoxy/SWCNT compared to that in epoxy/CF composite. The increase Young's modulus and structural change (from solid to hollow structure) contributed 69% and 31%, respectively to this enhancement (Figure 6b). Based on that, it could be seen that nano-fibers with higher aspect ratio and tensile properties can provide higher reinforcing efficiency compared to their micro-counterpart. Some researchers have claimed an equivalent or even higher strengthening effect could be achieved from using low loading of nano-fillers compared to that of micro-fillers. Fornes [51] indicated that the modulus of nylon 6 would be doubled by mixing only approximately 6.5 wt.% nano-clay montmorillonite (MMT) platelets whereas the same effect could be achieved when using three times volume of glass fiber or Campbell [52] claimed that a desired strength and stiffness of composite could be achieved when using 50 wt.% microparticles or 70 vt% of micro-fibers. Therefore, it could be seen that nanocomposites can provide excellent mechanical properties with low filler contents that can only be obtained using high filler content in conventional composites [53] since they proved as an efficient material to be used in demanding applications which require excellent strength to weight ratio. The improvement of stress transfer efficiency δ due to nanotube's diameter increase has also been confirmed by Li and Saigal [54] using shear-lag analysis and the representative volume element (RVE) (Figure 5d). In addition, they also considered the effect of fiber volume fraction as it has not been considered in previous studies.

The strengthening efficiency of nano-fillers such as CNT in MMNCs was also investigated and its mechanism is following load transfer [50], Orowan strengthening [55] and thermal expansion mismatch [56]. The strength improvement that is contributed by metal matrix grain size refinement [57], resulted from the addition of CNT has been found by [58]. Similar to polymer-based nanocomposites, the effect of reinforcement size also significantly contributed to strengthening behavior of MMNCs [59-61]. However, there were only a few models published that provided a comprehensive explanation of the strengthening mechanism of CNT reinforced MMNCs. Barai and Weng [62] have developed a two-scale model to analyze the elastoplastic behavior of CNT reinforced MMNCs that considered CNT agglomeration and interface properties as two main factors affecting the load transfer. Dong et al. [63] have built a dislocation model that combined the effect of both matrix grain size and filler size on the strengthening mechanism of metal/CNT nanocomposites (Figure 7). They claimed that the load transfer effect was improved at small grain size and high volume of CNT.

2.2 Mechanical properties of nanocomposites

From the discussions about the differences between nanocomposites and composites in the previous section, it could be intrinsically seen that reinforcing a matrix material by nano-fillers could lead to higher effectiveness of reinforcement than micro-fillers due to their advanced mechanical properties and novel nanostructures. Among many nano-fillers have been applied recently, CNTs, graphene and nano-clays are the most common reinforcing materials due to their compatibility and high efficiency of reinforcement with three main matrix materials including polymers, metals and ceramics. The major objective of the most relevant studies is to investigate the changes between the neat matrix and the matrix reinforced nano-fillers in terms of mechanical, thermal and electrical properties that are most common. Within the scope of this review, only the mechanical properties will be considered due to the requirements for the other sections related to the micromachining of nanocomposites. The effectiveness when reinforcing nano-fillers depends on many factors which can be classified into three main groups: (i) Nano-filler nature, (ii) Filler-matrix interaction and (iii) Fabricating methods.

2.2.1 CNT based nanocomposites

CNTs are allotropes of carbon that made of a cylindrical rolled-up single layer of the carbon atom. The diameters and lengths of CNTs range from 1-100 nm and 0.1 – 100 µm, respectively [64] with the tubular structure make them very high aspect ratio materials with the surface areas are in the range of 200–900 m^2/g [65]. CNT was first discovered by Iijima in the transmission electron microscopy (TEM) image in 1991 [66] and the first single-walled carbon nanotube was synthesized in 1993 by the same author [67]. Many applications have been found for CNT in different domains such as drug delivery [68], health care [69], electronics [70], electrics and thermal applications [71]. Due to their high strength-to-weight ratio, aspect ratio, thermal and electrical properties [72, 73], CNTs have found huge potential applications on composite reinforcement.

2.2.1.1 CNT reinforced polymer matrix nanocomposites

CNTs have been employed to reinforce polymers due to their better interfacial interaction in comparison to ceramic [74] or metal matrix [75] and the similar characteristic of organic structure. Therefore, it has been witnessed that there were some polymer/CNTs nanocomposites with tensile strengths ranging from 0.1 to 5 GPa and Young's modulus from 5 to 200 GPa [76]. Generally, the mechanical properties were improved when using CNTs as reinforcement in some polymers such as epoxy [77-80], polystyrene (PS) [81], polyethylene [82, 83], PMMA [84, 85], poly (p-phenylene benzobisoxazole) (PBO) [86], polyvinyl alcohol (PVA) [87], polyester elastomers (PEE) [88], polycarbonate (PC) [89], polyamide-6 [90] and nylon-6 [91]. The optimum loading of CNTs has to be considered carefully to avoid agglomerations or bundles that negatively affect the mechanical properties of PMNCs, usually when CNTs content exceeds 2-3% [92]. Figure 8 shows some improvements in terms of Young's moduli and tensile strengths when reinforcing polymer by CNTs with the corresponding dispersion techniques. Generally, it could be seen that the level of CNTs distribution in polymer matrixes, their interfacial interaction and processing methods significantly affect the load transfer from the matrix to CNTs, hence decide their effectiveness of reinforcement in terms of mechanical properties of polymer-based nanocomposites. From Figure 8, it was observed that both Young's modulus and tensile strength of nanocomposites improved with the addition of CNTs. However, there are different thresholds of CNTs loading at which the tensile strengths decrease or even lower than pristine polymers. It is possibly due to the re-agglomeration [93-95] of CNTs due to insufficient dispersion techniques, high loading of fillers hence creating the more stress concentration and reducing the effectiveness of CNT as reinforcement. Specifically, the poor interfacial interaction between CNT and polyester even leads to the negative influence on tensile strength of nanocomposite [96, 97]. In terms of dispersion methods, solution mixing, in situ polymerization dry mixing and melt mixing are the most common methods for fabricating polymer based nanocomposites. Esawi et al. [98] have investigated the effects of dispersion methods (dry mixing and solution mixing) on the mechanical properties of PP/CNT nanocomposites (Figure 9). The results have indicated a higher level of CNT distribution when using dry-mixing in comparison with solution-mixing. The degradation of the polymer, high viscosity due to the addition of solutions that limited the CNT distribution contributed to the lower improvements of mechanical properties when applying solution-mixing. In addition, employing ultra-sonication in solution-mixing might damage the CNT structure, hence also contributed to low mechanical properties of nanocomposites [99]. Associated with the effect of CNT content, the influence of CNT structure on the mechanical properties of CNT-based nanocomposites has been also indicated considerable. Since CNTs have various types: SWCNTs, double-walled CNTs (DWCNTs) and MWCNTs, their different structures and properties lead to various efficiencies in terms of mechanical reinforcement. Figure 10 shows the improvements in tensile properties when reinforcing epoxy with different types of CNTs. Theoretically, the addition of SWCNTs and DWCNTs exhibited higher reinforcement of mechanical properties than MWCNTs due to their higher mechanical properties, aspect ratio and specific surface area. In addition, the multi-layer structure of MWCNTs basically leads to the low effective surface area in comparison with less-layer structure CNTs. However, this reinforcing effectiveness also depends on how homogenous the CNTs distribute within the polymer matrix. In this case, DWCNTs showed no agglomeration as SWCNTs that explained for a higher improvement of tensile properties. This phenomenon was also verified by Fornes et al. [100] and Sennett et al. [101] that the dispersion of MWCNTs within PC matrix was much more effective than SWCNT regardless the fabricating routes. They explained that SWCNT had a high propensity to re-agglomerate during the synthesis making the exfoliation more difficult in comparison with MWCNT.

Besides the structure, CNTs alignment also has a dominant effect on the mechanical properties of polymer-based nanocomposites. This feature could be attained using several methods such as shear flows [102], ex-situ alignment [103], force field-induced alignment [104], magnetic field-induced alignment [105], electrospinning-induced alignment [106] and liquid crystalline phase-induced alignment [107].

Figure 11 shows some experimental results that exhibited the improvements of tensile properties of CNT based nanocomposites with aligned CNTs in comparison with non-aligned CNTs. It could be basically explained by the isotropic nature of nanocomposites when CNT alignment was employed and also leading to better distribution and reducing agglomeration of CNT when filling into the polymer matrix. In addition, functionalization has been considered as an effective treatment of CNTs to improve their interactive adhesions with polymer matrix, hence enhance the reinforcing effectiveness of mechanical properties through load transferring. Khare et al. [108] have indicated that reinforcing epoxy by amido-anime functionalized CNTs (f-CNTs) led to a higher improvement of mechanical properties in comparison with pristine-CNTs (p-CNTs) (~ 51% of Young’s modulus). Some main reasons were given including lower interphase compression, matrix structure integrity, suppression of matrix mobility, stable-covalent bonds of epoxy-FCNTs and subsequent facilitation of load transfer (Figure 12).

Unlike the improvements of tensile strength and Young’s modulus, the addition of CNTs exhibited different variations of fracture strain and toughness. Figure 13 shows the different trends of fracture strain improvement between thermoplastic and thermosetting reinforced by CNTs at various weight content. It could be seen that the flexibility of thermoplastic nanocomposites was significantly decreased at every filler loadings. Although relevant studies have shown this phenomenon, a comprehensive mechanism to explain it has been not proposed. Wang et al. [109] claimed that the degradation of flexibility when adding MWCNT-NH_2 into Polyimide (PI) was possibly due to strong interface interaction between matrix and filler. Consequently, the movement of polymer chains under loading could be restricted and hence, decreasing the flexibility of this material. However, the characterization of interfacial strength has not been made to support this claim. On the other hand, the fracture strains of thermosets could be enhanced by the addition of CNTs at certain levels of contents which is different from thermoplastic nanocomposites. When reinforcing epoxy by MWCNT, Chen et al. [110] indicated that the brittle epoxy phase was toughened by dispersed CNT. This enhancement of failure strain at certain low filler loadings (below 1 wt.%) was confirmed by Gojny et al. [111]. At higher CNT loadings, CNT agglomeration led to stress concentration and weaken the interfacial interaction of polymer-CNT, hence reducing the fracture strain. Scanning electron microscope (SEM) imaging was employed to demonstrate these explanations in terms of CNT distribution at different filler contents.

Regarding the fracture toughness, CNTs have been qualified as a potential reinforcing candidate to replace glass fiber (GF) or CF to attain higher toughening efficiency due to their high aspect ratio and stiffness [112]. The micro-mechanical toughening mechanism of polymer reinforced CNT nanocomposites can be expressed as follows: (1) crack bridging by CNTs and (2) CNTs de-bonding and pull-out or breaking depends on the interface strength and applied load [113, 114] (Figure 14). Based on this schematic, it could be seen that the highest fracture toughness could be achieved if CNTs are oriented transversely with the propagated cracks in which the bridging mechanism takes effect. Otherwise, it will not have considerable influence on fracture toughness in the case of longitudinal or random distribution of CNTs [115]. In addition, the effect of transverse alignment could be only effective at a low loading of CNTs. Some studies have shown a maximum enhancement of fracture toughness (around 51%) of polymer/CNT nanocomposites at 3 wt.% of fillers was used and decreased when exceeded this threshold due to filler agglomeration [115, 116]. On the other hand, the random distribution of CNTs did not show considerable enhancement in toughness at low filler content (< 1wt.%) [117]. In addition, Chen et al. [114] have analyzed the effect of CNT length and interface strength on fracture toughness. They claimed that the fracture toughness could not be improved with the consideration of interface chemical bond density or fiber length only but combined them together. The optimal values of these indicators were around 5-10% and 100 nm, respectively. Optimal CNT-bridging from their experiment has confirmed this theoretical analysis. Generally, reinforcing polymers by long CNT can achieve high fracture toughness due to its high load transfer and hence, improving the interface shear strength [118, 119]. The structure of CNTs has also influenced the fracture toughness of nanocomposites. Low contents of DWCNT (<0.5 wt.%) have shown a remarkable improvement of fracture toughness of epoxy-based nanocomposites due to its high compatibility with epoxy matrix (37). However, using suitable dispersion methods and functionalization could make MWCNT better reinforcing candidate to enhance fracture toughness than other types of CNTs (18). In general, the fracture toughness improvement when reinforcing polymer by CNTs has shown a complicated correlation between various factors including CNT content, structure, alignment, treatment as well processing technique. Table 3 shows some fracture toughness improvements of polymer reinforced CNT nanocomposites with the consideration of the aforementioned factors.

2.2.1.2 Carbon nanotube reinforced metal matrix nanocomposites

Although CNTs are theoretically considered an effective reinforcement for high strength-to-weight materials, few studies have concerned about using them to reinforce metals. The incorporation of CNTs in metals has some difficulties due to the inherent characteristics of both CNTs and metals, the fabricating conditions that negatively affect the interfacial adhesion as well as CNTs defects and subsequently, the improvement of mechanical properties of metal reinforced CNT nanocomposites. In general, there are two main challenges that hinder CNTs from achieving high effectiveness of reinforcement in the metal matrix. The first challenge is the poor interfacial adhesion between CNTs and metals. It is due to the nature of CNTs such as low compatibility with high surface energy (72.8 $mJ.m^{-2}$) [120] high surface tension (721 mN/m) [121], low wettability or hydrophobicity [122] and high possibility of agglomeration because of Van der Waals forces [123]. Because chemical bonding between CNT-metal is neglected, these physical factors are dominant in the interfacial interaction [121]. Secondly, the undesirable chemical reactions between CNTs and metals at high temperature, pressure from fabricating conditions such as sintering, hot milling. It leads to the formation of intermetallic such as Al_4C_3 [124], TiC [125], Al_2MgC_2 [126]. Generally, a minor formation of carbide can positively improve the interfacial adhesion while an uncontrolled process could lead to serious damages of CNTs and in situ carbide formations [127, 128] or enhance CNTs amorphization as well as their thermal decomposition [129]. Some solutions have been adapted to improve the wettability and distribution of CNTs as well as their interfacial strength with metal matrix such as chemical functionalization [130], surfactant [131], coating CNTs with Ni [132, 133], Si [134] or in situ synthesis CNTs within metal matrix [135]. In general, some main improvements in terms of tensile properties and hardness when reinforcing metals by CNTs are shown in Table 4. The effectiveness of the improvement of mechanical properties of metals reinforced CNTs depends on the homogenous distribution of CNTs [132, 136-139], interfacial strength of metal/CNT [132, 133, 139, 140], thermal expansion mismatch between metal and CNTs [141], grain refinement effect [133, 142], CNTs structure retention of plastic deformations of metal matrixes [132, 139, 140, 143], that all contributed to strengthening mechanism. The two last ones also contribute to the hardness improvement of metal/CNT nanocomposites.

2.2.2 Graphene-based nanocomposites

Graphene is a planar sheet of a single layer of sp^2-bonded carbon atoms that is considered as an original structure element of other carbon allotropes such as CNTs, graphite and diamond. This two-dimensional (2D) structure provides graphene with a much larger specific surface area of ~ 2600 m^2/g than other carbon allotropes such as carbon black (CB) or CNTs [144]. Graphene exhibits exceptional mechanical properties such as Young's modulus (~1 TPa) or strength (130 GPa) [145] hence considered as the strongest material [145]. Moreover, this material is also an excellent conductor with high thermal and electrical conductivity of ~4000 WmK^{-1} [146] and ~ 6000 $S.cm^{-1}$ [147], respectively and other properties such as gas impermeability, optical transmittance. Therefore, graphene has high potential in a wide range of applications such as flexible electronic devices, transparent coating material, energy storage, and especially, nanocomposites [148-150].

2.2.2.1 Graphene reinforced polymer matrix nanocomposites

Many researchers have attempted to investigate the reinforcing efficiency of graphene in nanocomposites by considering various factors such as the effective modulus, filler dispersion [151], alignment [152], agglomeration [153] or fabricating methods [11]. All of these factors have certain influences on the filler distribution and graphene-matrix interfacial adhesion or stress transfer that subsequently affect the reinforcing effectiveness of graphene-based fillers.

The effective modulus of thermal expanded graphite oxide (TEGO) has been measured when it was mixed with PC and polyethylene. Only a slight improvement of modulus was experimentally observed in comparison with graphite-based composites while its effective modulus was around 70 GPa-7% of the value for defect-free graphene (~1 TPa) [154, 155]. This low effective modulus of graphene is explained by its wrinkled geometry once dispersed in the matrix [156], which consequently unfold under tensile load instead of stretching. The incomplete exfoliation could also lead to the aspect ratio reduction of graphene [51] that contributes to this phenomenon.

Graphene-matrix interfacial adhesion is considered as another crucial factor that affects the effective reinforcement [157, 158] since it makes ineffective dispersion as well as load transfer, hence resulting in a low modulus of nanocomposites [159]. Some significant increases of composite tensile moduli were observed when using graphene as reinforcement due to the roughness of the platelets [160] that attribute to mechanical interlocking within the matrix and hence, strong interfacial bonding.

In addition, the reinforcing effectiveness of graphene also depends on the processing method. For instance, melt mixing has been found less suitable in graphene-based nanocomposites since this method causes particle attrition [161] that possibly decrease the filler ratio. In situ polymerization, on the other hand, can generate good dispersion but it also causes polymer chain extension by graphene, resulting in a less modulus improvement of composites than solution-mixing method [11]. This comparison between different processing methods can be seen in Figure 15.

Table 5 summarizes some improvements in mechanical properties when reinforcing polymers with graphene. In general, the elastic moduli increased with the addition of graphene while the tensile strengths decreased. It is explained by the improvement of interfacial interaction of matrix-filler due to the high aspect ratio of graphene [162] that effectively bridging with the matrix molecules and leading to a high stiffening effect [163]. As a consequence, the tensile strength of nanocomposites would be reduced. Moreover, this reduction is also due to the fabricating methods, re-agglomeration of graphene that constitutes some defects in the polymer matrix. The presence of graphene also opposes the flow of amorphous phase and increase the crystallization of hard segment of a polymer matrix that subsequently contributes to the elastic modulus improvement and the tensile strength reduction of polymer-based nanocomposites [164].

Similar to CNTs, the addition of graphene into the polymer matrix leads to different variations in terms of fracture strain and toughness. Fracture strain showed a significant reduction in the case of thermoplastic/graphene nanocomposite while this property was improved for thermoset plastic reinforced with low loading of graphene (Figure 16). However, the fracture toughness improvement when using graphene seems to be higher than CNT. Domun et al. [165] have collected experimental values of fracture toughness when using graphene to reinforce epoxy from relevant studies (Figure 17). They claimed that among common nano-fillers (CNTs, graphene, and nano-clay), graphene exhibited higher fracture toughness enhancement in epoxy-based nanocomposites, mostly at low filler loadings (<1 wt.%). It is due to the higher surface area, aspect ratio of graphene, as well as its exceptional stiffness and strength, compared to CNT as aforementioned. Rafiee et al [166]., in a comparative study, have claimed that graphene exhibited better mechanical reinforcement including Young's modulus, tensile strength and toughness than MWCNT. It was due to poor interfacial contact area, wetting and adhesion of MWCNT that showed ineffective reinforcing epoxy-based nanocomposites. On the other hand, higher aspect ratio allowed more interfacial contact between graphene and epoxy matrix in contrast with the only outer tube of MWCNT. In addition, wrinkled sheets of graphene also contributed to better interfacial binding, hence improving the toughening mechanism in epoxy/graphene nanocomposites. The micro-mechanical toughening mechanism of polymer reinforced graphene is also different from that in CNTs. While filler pull-out and de-bonding still exhibit along the cracks, there is no presence of graphene cracking. When the crack reaches to the graphene surface, it will be deflected and bifurcated then propagating around the filler. The ease of shearing between graphene sheets also allows the crack propagation goes through or penetrates within layers (Figure 18).

2.2.2.2 Graphene reinforced metal matrix nanocomposites

Graphene has been also applied to reinforce metal with the aim to improve their stiffness but subsequently leads to the reduction of ductility that was called 'strengthening mechanism'. However, tensile strengths have been found an increase in some cases [167-169] possibly due to the straightening of wrinkled graphene during the plastic deformation or ball milling process [170]. In general, the strengthening mechanism is related to the improvements of yield strength [171], elongation [168], flexural strength [172], but Young's modulus and hardness are most fundamental objectives. The improvements of Young's modulus when reinforcing metal with graphene is ascribed to the homogenous distribution of graphene [173], compact interfacial bonding of metal-graphene [174] that lead to effective load transfer [175]. On the other hand, the improvements of hardness in nanocomposites are possibly due to the mismatch of thermal expansion coefficient [176] between graphene and metal matrix as well as the restriction or obstruction of graphene in plastic deformation [177-180]. In addition, the formation of metal carbide due to the chemical reaction between graphene and metal during synthesis contributes to the strengthening effectiveness. Al carbide (Al_4C_3) has been observed in Al/graphene nanocomposite synthesis using hot extrusion [171]. However, its role in terms of improvement of hardness has been still controversial whether it leads to the reduction of strength, hardness [171] or enhancement of bonding strength, load transfer [181]. The interfacial reaction can be improved by the formation of carbide because it decreases the contact angle of liquid alloy hence increase the wetting [180]. Furthermore, using metal powder through ball milling and sintering processes in high temperature can cause oxidation or the formation of metal oxide. Song et al. [182] reported that the hardness of Cu/ graphene nanocomposite was improved due to the presence of Cu_2O during the synthesis but it was reduced when increasing graphene loading. Similarly, Lin et al. [180] indicated that the formation of Fe_3C after sintering decreased the contact angle between liquid-alloy and GO, hence increasing GO wettability (Figure 19). In case no carbide is formed, the interfacial bonding of metal-graphene strongly depends on matrix nature (contact angle and cohesive energy of liquid-metal and filler) that has been addressed in case of Mg matrix [183]. Hwang et al. [184] have confirmed the compatibility between Mg and graphene with their high adhesion energy. In addition, pre-coating metals such as Ni on graphene surfaces have shown similar effects on improving the wettability of fillers in the Cu matrix [185] as compared to CNT cases [186]. Xu and Buehler [187] have pointed out that Ni-graphene has higher cohesive energy and interfacial strength than Cu-graphene.

In general, the improvements of mechanical properties of metal/graphene nanocomposites have shown their dependences on integrity of graphene [172], graphene exfoliation [188] and distribution [173], interfacial bonding [172], prevention of metal dislocation [179] beside the aforementioned roles of intermetallic formation due to sintering process (Table 6). These formations of metal carbide, metal oxide through the synthesis might contribute to these improvements but cannot be evaluated whether they have positive or negative effects on mechanical properties of graphene reinforced metal nanocomposites.

2.2.3 Ceramic based nanocomposites

In this section, the other nano-filler based nanocomposites will be reviewed in terms of their mechanical properties. There were many types of nano-fillers instead of CNTs and graphene that make the discussion in details for all of them not feasible within the scope of this review section. Therefore, some common nano-filler based nanocomposites will be taken into consideration including polymer/nano-clay, polymer/ceramic and metal/ceramic nanocomposites. These selections are also based on the effective reinforcements of nano-fillers with their corresponding matrices as well as their important applications as engineering materials.

Beside of CNTs and graphene, nano-clay and ceramic nanoparticles have also been applied as reinforcement in polymer materials due to their advanced tensile properties. Nanoclays are potential candidates for nanocomposite reinforcements, especially in terms of mechanical properties. The most common type of nanoclays has been applied in reinforcing nanocomposites is montmorillonite (MMT). It is derived from absorbent aluminum phyllosilicate clay called" bentonite" and thus named "organoclays". MMT has been applied for reinforcing polymers due to their high aspect ratio and unique intercalation/exfoliation natures [189]. The incorporation of organoclays into polymer matrices has exhibited superior strength and modulus [190]. The most applied polymers by nanoclay reinforcements are polystyrene [191], epoxy resin [192], poly(methyl methacrylate) [193], poly(ε-caprolactone) [194], PP [195], polyurethanes [196], polyimides [197]. However, nanoclays mostly require pre-exfoliation to attain homogenous distribution due to higher specific area and hence higher effective of load transfer could be achieved [198]. In general, the effectiveness of nanoclay reinforcements have been indicated strongly depend on intercalation methods [199], exfoliation nanoclays [200-202], the integrity of nanoclays [203] or matrices [204], and most importantly, the level of distribution of nanoclays [205] or interaction of polymer-nanoclays [201, 205]. However, the addition of nanoclays in polymer exhibited some negative effects on tensile strength of nanocomposites in some cases but no explanation was given [205].

On the other hands, silica nano-particles are also common nano-fillers that have been applied to reinforce polymers due to their high mechanical properties. The processing methods to fabricate these materials are similar to other polymer-based nanocomposites such as melt mixing for PP (63), PE (71n), PEN (62), PET (102), solution mixing for epoxy [206], poly(4-methyl-2-pentyne) (PMP) (123, 124), or sol-gel processing for epoxy [207]. In general, the additions of nano-silica in polymer matrices lead to the improvements of stiffness mostly due to the homogenous distribution, high aspect ratio and stiffness of silica nano-particles. However, it could be seen that their effectiveness of stiffness improvement are not high as CNTs, graphene or nano-clays (Table 7).

In the case of ceramic reinforced MMNCs, the main challenge is the incorporation of ceramic nano-particles into molten metal matrices due to their poor wettability. Besides high wetting could be seen in some metal/ceramic systems with strong (chemical) reactions and low contact angles (θ) such as Cu/WC ($\theta = 20^0$) or Au/ZrB_2 ($\theta = 25^0$), most of the other ceramic nano-fillers generate non-covalent (physical) bonds with liquid metals with low wettability such as Ag/Al_2O_3, Cu/SiO_2 ($\theta = 120°–140°$); Au/BN($\theta = 135°–150°$) at high temperature [208]. The inhomogeneous distribution of ceramic nano-particles and their agglomerations within metal matrix have been indicated resulting from their low wettability associated with high specific surface areas. Some dispersion routes have been employed to overcome these obstacles including ex-situ and in-situ techniques [209]. The basic difference between these two methods is whether the reinforcements (ceramic nano-particles) are fabricated within the matrices (in-situ) [210] or separately synthesized outside by CVD [211], spray conversion process [212] or laser-induced gas-phase reaction [213] and then subsequently incorporated into metal matrices via powder metallurgy (PM) [214] or mechanical alloying (MA) [215]. Although the traditional PM method has been successfully applied to synthesis metal/ceramic nanocomposites, especially in aluminium-based matrices, it still exhibited obvious agglomerations of ceramic nano-particles and hence their inhomogeneous distribution [216, 217] (Figure 20). The low wettability of as-produced ceramic nano-particles, as well as their high specific surface area, have indicated the main reasons for this drawback. It could be improved by employing MA methods with better dispersion of ceramic nano-fillers with significant grain size reduction [218, 219]. In addition, the densification of MA is mainly conducted by hot pressing, HIP or extrusion. On the other hand, In-situ route has been claimed more suitable than the aforementioned methods in terms of generating the homogenous distribution of ceramic nano-particles such as Al_3Ti [220] or TiC [221] at high loadings (50 vol.% and 18 vol.%, respectively) and subsequent ultrafine microstructures. In general, the additions of ceramic nano-particles lead to the improvements of tensile strength, yield strength and hardness associated with the sacrifice of ductility. All these changes in tensile properties follow strengthening mechanisms including Orowan strengthening, mismatch of thermal expansion coefficients between matrix and filler (CTE) and grain size refinement. In addition, the reductions of ductility have been claimed due to the presence of porosities within the system or brittle nano-fillers [216, 222] although some improvements of ductility could be seen when using Mg-based matrices [223, 224] without sufficient explanation. The role of ceramic nano-fillers on hindering the matrix dislocations and the effect of grain size reduction have discussed in most relevant researches that were the main reasons for hardness increments [216, 222, 223, 225-228]. Table 8 summarizes the mechanical properties of some common ceramic nano-particles reinforced MMNCs with their corresponding fabricating methods and discussion.

3. CONCLUSIONS

The first part of this paper has addressed relevant studies including the fabrication and characterization of nanocomposites. Based on that, it has been observed that the addition of nano-fillers as reinforcement improved mechanical properties of nanocomposites. The level of enhancement depends on many factors such as the nature of both filler and matrix, their interaction, filler size and fabricating methods. Strenthening and toughening mechanisms were also employed to explain these variations via modelling and experimental approaches. This review paper has focused on nanocomposite materials that require mechanical micromachining processes in order to produce the final product. These include polymer/CNT, polymer/graphene and metal/ceramic nanocomposites. This part of the review will be the basis to analyse the machinability of nanocomposites when employing mechanical micromachining techniques where the mechanical properies will be correlated with different machining measures.

REFERENCES

[1] A. Blumstein, "ETUDE DES POLYMERISATIONS EN COUCHE ADSORBEE. 1," *Bulletin de la Societe Chimique de France,* pp. 899-&, 1961.

[2] A. Blumstein, "Polymerization of adsorbed monolayers. II. Thermal degradation of the inserted polymer," *Journal of Polymer Science Part A: General Papers,* vol. 3, pp. 2665-2672, 1965.

[3] I. Arora, J. Samuel, and N. Koratkar, "Experimental investigation of the machinability of epoxy reinforced with graphene platelets," *Journal of Manufacturing Science and Engineering,* vol. 135, p. 041007, 2013.

[4] I. Srikantha, P. Ghosalb, A. Kumara, and R. Jaina, "Nanocomposites for Aerospace Applications," *Nanotech,* p. 52.

[5] J. M. Garces, D. J. Moll, J. Bicerano, R. Fibiger, and D. G. McLeod, "Polymeric nanocomposites for automotive applications," *Advanced Materials,* vol. 12, pp. 1835-1839, 2000.

[6] D. Feldman, "Polymer nanocomposites in medicine," *Journal of Macromolecular Science, Part A,* vol. 53, pp. 55-62, 2016.

[7] I. Dinca, C. Ban, A. Stefan, and G. Pelin, "Nanocomposites as advanced materials for aerospace industry," *Incas Bulletin,* vol. 4, p. 73, 2012.

[8] A. Leszczyńska, J. Njuguna, K. Pielichowski, and J. Banerjee, "Polymer/montmorillonite nanocomposites with improved thermal properties: Part I. Factors influencing thermal stability and mechanisms of thermal stability improvement," *Thermochimica acta,* vol. 453, pp. 75-96, 2007.

[9] J. Bai and A. Allaoui, "Effect of the length and the aggregate size of MWNTs on the improvement efficiency of the mechanical and electrical properties of nanocomposites—experimental investigation," *Composites Part A: applied science and manufacturing,* vol. 34, pp. 689-694, 2003.

[10] N. Dong, M. Zhong, P. Fei, Z. Lei, and B. Su, "Magnetic and electrochemical properties of PANI-CoFe2O4 nanocomposites synthesized via a novel one-step solvothermal method," *Journal of Alloys and Compounds,* vol. 660, pp. 382-386, 2016.

[11] H. Kim, Y. Miura, and C. W. Macosko, "Graphene/polyurethane nanocomposites for improved gas barrier and electrical conductivity," *Chemistry of Materials,* vol. 22, pp. 3441-3450, 2010.

[12] Y. Liu, W. Xiong, L. Jiang, Y. Zhou, and Y. Lu, "Precise 3D printing of micro/nanostructures using highly conductive carbon nanotube-thiol-acrylate composites," in *Laser 3D Manufacturing III*, 2016, p. 973808.

[13] Q. Y. Tang, Y. C. Chan, N. B. Wong, and R. Cheung, "Surfactant-assisted processing of polyimide/multiwall carbon nanotube nanocomposites for microelectronics applications," *Polymer International,* vol. 59, pp. 1240-1245, 2010.

[14] F.-C. Chen, C.-W. Chu, J. He, Y. Yang, and J.-L. Lin, "Organic thin-film transistors with nanocomposite dielectric gate insulator," *Applied physics letters,* vol. 85, pp. 3295-3297, 2004.

[15] H. Tang and H. A. Sodano, "High energy density nanocomposite capacitors using non-ferroelectric nanowires," *Applied Physics Letters,* vol. 102, p. 063901, 2013.

[16] P. M. Raj, H. Sharma, G. P. Reddy, N. Altunyurt, M. Swaminathan, R. Tummala*, et al.*, "Cobalt–polymer nanocomposite dielectrics for miniaturized antennas," *Journal of electronic materials,* vol. 43, pp. 1097-1106, 2014.

[17] E. Goossen, "Vertical take off and landing unmanned aerial vehicle airframe structure," ed: Google Patents, 2012.

[18] D. J. Pines and F. Bohorquez, "Challenges facing future micro-air-vehicle development," *Journal of aircraft,* vol. 43, pp. 290-305, 2006.

[19] R. Vijayanandh, N. Kumar, S. Kumar, R. Kumar, and N. Kumar, "Material Optimization of High Speed Micro Aerial Vehicle using FSI Simulation," *Procedia Computer Science,* vol. 133, pp. 2-9, 2018.

[20] D. Kumar, T. Goyal, V. Kumar, P. Mohite, S. Kamle, and V. Verma, "Development and modal analysis of bioinspired CNT/epoxy nanocomposite MAV flapping wings," *J. Aerosp. Sci. Technol,* vol. 67, pp. 88-93, 2015.

[21] X. Sun and J. Li, "Friction and wear properties of electrodeposited nickel–titania nanocomposite coatings," *Tribology Letters,* vol. 28, pp. 223-228, 2007.

[22] M. Imbaby and K. Jiang, "Fabrication of free standing 316-L stainless steel–Al2O3 composite

micro machine parts by soft moulding," *Acta Materialia,* vol. 57, pp. 4751-4757, 2009.

[23] M. Imbaby and K. Jiang, "Stainless steel–titania composite micro gear fabricated by soft moulding and dispersing technique," *Microelectronic Engineering,* vol. 87, pp. 1650-1654, 2010.

[24] I. Timoshkov, V. Kurmashev, and V. Timoshkov, "Electroplated nanocomposites of high wear resistance for advanced systems application," in *Advances in Nanocomposite Technology*, ed: IntechOpen, 2011.

[25] R. N. Das, F. D. Egitto, J. M. Lauffer, and V. R. Markovich, "Laser micromachining of nanocomposite-based flexible embedded capacitors," in *2007 Proceedings 57th Electronic Components and Technology Conference*, 2007, pp. 435-441.

[26] E. N. Udofia and W. Zhou, "A guiding framework for microextrusion additive manufacturing," *Journal of Manufacturing Science and Engineering,* vol. 141, 2019.

[27] T. Bartkowiak and C. A. Brown, "A Characterization of Process–Surface Texture Interactions in Micro-Electrical Discharge Machining Using Multiscale Curvature Tensor Analysis," *Journal of Manufacturing Science and Engineering,* vol. 140, 2018.

[28] J. Li, J. Liu, J. Liu, Y. Ji, and C. Xu, "Experimental investigation on the machinability of SiC nano-particles reinforced magnesium nanocomposites during micro-milling processes," *International Journal of Manufacturing Research,* vol. 8, pp. 64-84, 2013.

[29] E. Brinksmeier, R. Gläbe, O. Riemer, and S. Twardy, "Potentials of precision machining processes for the manufacture of micro forming molds," *Microsystem Technologies,* vol. 14, p. 1983, 2008.

[30] M. Huang and Z. Li, "Influences of particle size and interface energy on the stress concentration induced by the oblate spheroidal particle and the void nucleation mechanism," *International journal of solids and structures,* vol. 43, pp. 4097-4115, 2006.

[31] W. Zhou, D. Yu, C. Wang, Q. An, and S. Qi, "Effect of filler size distribution on the mechanical and physical properties of alumina-filled silicone rubber," *Polymer Engineering & Science,* vol. 48, pp. 1381-1388, 2008.

[32] N. Chisholm, H. Mahfuz, V. K. Rangari, A. Ashfaq, and S. Jeelani, "Fabrication and mechanical characterization of carbon/SiC-epoxy nanocomposites," *Composite structures,* vol. 67, pp. 115-124, 2005.

[33] M. Dekkers and D. Heikens, "The effect of interfacial adhesion on the tensile behavior of polystyrene–glass-bead composites," *Journal of Applied Polymer Science,* vol. 28, pp. 3809-3815, 1983.

[34] Q. Zhang, M. Tian, Y. Wu, G. Lin, and L. Zhang, "Effect of particle size on the properties of Mg (OH) 2-filled rubber composites," *Journal of Applied Polymer Science,* vol. 94, pp. 2341-2346, 2004.

[35] K. Radford, "The mechanical properties of an epoxy resin with a second phase dispersion," *Journal of Materials Science,* vol. 6, pp. 1286-1291, 1971.

[36] J. Spanoudakis and R. Young, "Crack propagation in a glass particle-filled epoxy resin," *Journal of Materials Science,* vol. 19, pp. 473-486, 1984.

[37] Y. Nakamura, M. Yamaguchi, M. Okubo, and T. Matsumoto, "Effect of particle size on mechanical properties of epoxy resin filled with angular-shaped silica," *Journal of applied polymer science,* vol. 44, pp. 151-158, 1992.

[38] A. Lazzeri, Y. Thio, and R. Cohen, "Volume strain measurements on CaCO3/polypropylene particulate composites: the effect of particle size," *Journal of applied polymer science,* vol. 91, pp. 925-935, 2004.

[39] N. Suprapakorn, S. Dhamrongvaraporn, and H. Ishida, "Effect of CaCO3 on the mechanical and rheological properties of a ring-opening phenolic resin: Polybenzoxazine," *Polymer composites,* vol. 19, pp. 126-132, 1998.

[40] R. Singh, M. Zhang, and D. Chan, "Toughening of a brittle thermosetting polymer: effects of reinforcement particle size and volume fraction," *Journal of materials science,* vol. 37, pp. 781-788, 2002.

[41] A. Roulin-Moloney, W. Cantwell, and H. Kausch, "Parameters determining the strength and toughness of particulate-filled epoxy resins," *Polymer composites,* vol. 8, pp. 314-323, 1987.

[42] G. C. Onuegbu and I. O. Igwe, "The effects of filler contents and particle sizes on the mechanical and end-use properties of snail shell powder filled polypropylene," *Materials Sciences and Applications,* vol. 2, p. 810, 2011.

[43] D. Devaprakasam, P. Hatton, G. Möbus, and B. Inkson, "Effect of microstructure of nano-and micro-particle filled polymer composites on their tribo-mechanical performance," in *Journal of Physics: Conference Series*, 2008, p. 012057.

[44] D. Edwards, "Polymer-filler interactions in rubber reinforcement," *Journal of Materials Science,* vol. 25, pp. 4175-4185, 1990.

[45] O. Kamigaito, "What can be improved by nanometer composites?," *Journal of the Japan Society of Powder and Powder Metallurgy,* vol. 38, pp. 315-321, 1991.

[46] R. M. Kumar, S. K. Sharma, B. M. Kumar, and D. Lahiri, "Effects of carbon nanotube aspect ratio on strengthening and tribological behavior of ultra high molecular weight polyethylene composite," *Composites Part A: Applied Science and Manufacturing,* vol. 76, pp. 62-72, 2015.

[47] S. Chowdhury and T. Okabe, "Computer simulation of carbon nanotube pull-out from polymer by the molecular dynamics method," *Composites Part A: Applied Science and Manufacturing,* vol. 38, pp. 747-754, 2007.

[48] K. Yazdchi and M. Salehi, "The effects of CNT waviness on interfacial stress transfer characteristics of CNT/polymer composites," *Composites Part A: Applied Science and Manufacturing,* vol. 42, pp. 1301-1309, 2011.

[49] K. Xiao and L. Zhang, "The stress transfer efficiency of a single-walled carbon nanotube in epoxy matrix," *Journal of Materials Science,* vol. 39, pp. 4481-4486, 2004.

[50] H. Cox, "The elasticity and strength of paper and other fibrous materials," *British journal of applied physics,* vol. 3, p. 72, 1952.

[51] T. Fornes and D. Paul, "Modeling properties of nylon 6/clay nanocomposites using composite theories," *polymer,* vol. 44, pp. 4993-5013, 2003.

[52] F. C. Campbell, *Structural composite materials*: ASM international, 2010.

[53] A. Bhattacharya, K. Ganguly, A. De, and S. Sarkar, "A new conducting nanocomposite—PPy-zirconium (IV) oxide," *Materials research bulletin,* vol. 31, pp. 527-530, 1996.

[54] K. Li and S. Saigal, "Micromechanical modeling of stress transfer in carbon nanotube reinforced polymer composites," *Materials Science and Engineering: A,* vol. 457, pp. 44-57, 2007.

[55] S. Yoo, S. Han, and W. Kim, "Strength and strain hardening of aluminum matrix composites with randomly dispersed nanometer-length fragmented carbon nanotubes," *Scripta Materialia,* vol. 68, pp. 711-714, 2013.

[56] H. Choi, B. Min, J. Shin, and D. Bae, "Strengthening in nanostructured 2024 aluminum alloy and its composites containing carbon nanotubes," *Composites Part A: Applied Science and Manufacturing,* vol. 42, pp. 1438-1444, 2011.

[57] K. M. Youssef, R. O. Scattergood, K. L. Murty, J. A. Horton, and C. C. Koch, "Ultrahigh strength and high ductility of bulk nanocrystalline copper," *Applied Physics Letters,* vol. 87, p. 091904, 2005.

[58] D. H. Nam, S. I. Cha, B. K. Lim, H. M. Park, D. S. Han, and S. H. Hong, "Synergistic strengthening by load transfer mechanism and grain refinement of CNT/Al–Cu composites," *Carbon,* vol. 50, pp. 2417-2423, 2012.

[59] M. Ashby, "The deformation of plastically non-homogeneous materials," *The Philosophical Magazine: A Journal of Theoretical Experimental and Applied Physics,* vol. 21, pp. 399-424, 1970.

[60] C.-W. Nan and D. Clarke, "The influence of particle size and particle fracture on the elastic/plastic deformation of metal matrix composites," *Acta materialia,* vol. 44, pp. 3801-3811, 1996.

[61] D. Lloyd, "Particle reinforced aluminium and magnesium matrix composites," *International materials reviews,* vol. 39, pp. 1-23, 1994.

[62] P. Barai and G. J. Weng, "A theory of plasticity for carbon nanotube reinforced composites," *International Journal of Plasticity,* vol. 27, pp. 539-559, 2011.

[63] S. Dong, J. Zhou, D. Hui, Y. Wang, and S. Zhang, "Size dependent strengthening mechanisms in carbon nanotube reinforced metal matrix composites," *Composites Part A: Applied Science and Manufacturing,* vol. 68, pp. 356-364, 2015.

[64] B. Han, S. Sun, S. Ding, L. Zhang, X. Yu, and J. Ou, "Review of nanocarbon-engineered multifunctional cementitious composites," *Composites Part A: Applied Science and Manufacturing,* vol. 70, pp. 69-81, 2015.

[65] X.-L. Xie, Y.-W. Mai, and X.-P. Zhou, "Dispersion and alignment of carbon nanotubes in polymer matrix: a review," *Materials science and engineering: R: Reports,* vol. 49, pp. 89-112, 2005.

[66] S. Iijima, "Helical microtubules of graphitic carbon," *nature,* vol. 354, p. 56, 1991.

[67] S. Iijima and T. Ichihashi, "Single-shell carbon nanotubes of 1-nm diameter," *nature,* vol. 363, p. 603, 1993.

[68] B. Singh, C. Baburao, V. Pispati, H. Pathipati, N. Muthy, S. Prassana*, et al.*, "Carbon nanotubes. A novel drug delivery system," *International Journal of Research in Pharmacy and Chemistry,* vol. 2, pp. 523-532, 2012.

[69] S. Kumar, R. Rani, N. Dilbaghi, K. Tankeshwar, and K.-H. Kim, "Carbon nanotubes: a novel material for multifaceted applications in human healthcare," *Chemical society reviews,* vol. 46, pp. 158-196, 2017.

[70] L.-M. Peng, Z. Zhang, and S. Wang, "Carbon nanotube electronics: recent advances," *Materials today,* vol. 17, pp. 433-442, 2014.

[71] M. F. De Volder, S. H. Tawfick, R. H. Baughman, and A. J. Hart, "Carbon nanotubes: present and future commercial applications," *science,* vol. 339, pp. 535-539, 2013.

[72] H. Cebeci, R. G. de Villoria, A. J. Hart, and B. L. Wardle, "Multifunctional properties of high volume fraction aligned carbon nanotube polymer composites with controlled morphology," *Composites Science and Technology,* vol. 69, pp. 2649-2656, 2009.

[73] A. Allaoui, S. Bai, H.-M. Cheng, and J. Bai, "Mechanical and electrical properties of a MWNT/epoxy composite," *Composites science and technology,* vol. 62, pp. 1993-1998, 2002.

[74] S. S. Samal and S. Bal, "Carbon nanotube reinforced ceramic matrix composites-a review," 2008.

[75] N. Silvestre, "State-of-the-art review on carbon nanotube reinforced metal matrix composites," *International Journal of Composite Materials,* vol. 3, pp. 28-44, 2013.

[76] W. Lu, M. Zu, J. H. Byun, B. S. Kim, and T. W. Chou, "State of the art of carbon nanotube fibers: opportunities and challenges," *Advanced materials,* vol. 24, pp. 1805-1833, 2012.

[77] X. Gong, J. Liu, S. Baskaran, R. D. Voise, and J. S. Young, "Surfactant-assisted processing of carbon nanotube/polymer composites," *Chemistry of materials,* vol. 12, pp. 1049-1052, 2000.

[78] Y. Breton, S. Delpeux, R. Benoit, J. Salvetat, C. Sinturel, F. Beguin*, et al.*, "Functionalization of multiwall carbon nanotubes: properties of nanotubes-epoxy composites," *Molecular Crystals and Liquid Crystals,* vol. 387, pp. 135-140, 2002.

[79] J. Zhu, H. Peng, F. Rodriguez-Macias, J. L. Margrave, V. N. Khabashesku, A. M. Imam*, et al.*, "Reinforcing epoxy polymer composites through covalent integration of functionalized nanotubes," *Advanced Functional Materials,* vol. 14, pp. 643-648, 2004.

[80] J. Zhu, J. Kim, H. Peng, J. L. Margrave, V. N. Khabashesku, and E. V. Barrera, "Improving the dispersion and integration of single-walled carbon nanotubes in epoxy composites through functionalization," *Nano letters,* vol. 3, pp. 1107-1113, 2003.

[81] R. Haggenmueller, W. Zhou, J. Fischer, and K. Winey, "Production and characterization of polymer nanocomposites with highly aligned single-walled carbon nanotubes," *Journal of nanoscience and nanotechnology,* vol. 3, pp. 105-110, 2003.

[82] W. Tang, M. H. Santare, and S. G. Advani, "Melt processing and mechanical property characterization of multi-walled carbon nanotube/high density polyethylene (MWNT/HDPE) composite films," *Carbon,* vol. 41, pp. 2779-2785, 2003.

[83] Y. Bin, M. Kitanaka, and D. Zhu, "Flow-induced properties ofnanotube-filled polymer materials," *Macromolecules,* vol. 36, pp. 213-6, 2003.

[84] J. Zeng, B. Saltysiak, W. Johnson, D. A. Schiraldi, and S. Kumar, "Processing and properties of poly (methyl methacrylate)/carbon nano fiber composites," *Composites Part B: Engineering,* vol. 35, pp. 173-178, 2004.

[85] C. A. Cooper, D. Ravich, D. Lips, J. Mayer, and H. D. Wagner, "Distribution and alignment of carbon nanotubes and nanofibrils in a polymer matrix," *Composites science and technology,* vol. 62, pp. 1105-1112, 2002.

[86] S. Kumar, T. D. Dang, F. E. Arnold, A. R. Bhattacharyya, B. G. Min, X. Zhang*, et al.*, "Synthesis, structure, and properties of PBO/SWNT Composites&," *Macromolecules,* vol. 35, pp. 9039-9043, 2002.

[87] M. Paiva, B. Zhou, K. Fernando, Y. Lin, J. Kennedy, and Y.-P. Sun, "Mechanical and morphological characterization of polymer–carbon nanocomposites from functionalized carbon nanotubes," *Carbon,* vol. 42, pp. 2849-2854, 2004.

[88] Z. Roslaniec, G. Broza, and K. Schulte, "Nanocomposites based on multiblock polyester elastomers (PEE) and carbon nanotubes (CNT)," *Composite Interfaces,* vol. 10, pp. 95-102,

2003.

[89] P. Pötschke, A. R. Bhattacharyya, A. Janke, and H. Goering, "Melt mixing of polycarbonate/multi-wall carbon nanotube composites," *Composite Interfaces,* vol. 10, pp. 389-404, 2003.

[90] O. Meincke, D. Kaempfer, H. Weickmann, C. Friedrich, M. Vathauer, and H. Warth, "Mechanical properties and electrical conductivity of carbon-nanotube filled polyamide-6 and its blends with acrylonitrile/butadiene/styrene," *Polymer,* vol. 45, pp. 739-748, 2004.

[91] T. Liu, I. Y. Phang, L. Shen, S. Y. Chow, and W.-D. Zhang, "Morphology and mechanical properties of multiwalled carbon nanotubes reinforced nylon-6 composites," *Macromolecules,* vol. 37, pp. 7214-7222, 2004.

[92] D. Bikiaris, "Microstructure and properties of polypropylene/carbon nanotube nanocomposites," *Materials,* vol. 3, pp. 2884-2946, 2010.

[93] M. M. Shokrieh, A. Saeedi, and M. Chitsazzadeh, "Mechanical properties of multi-walled carbon nanotube/polyester nanocomposites," *Journal of Nanostructure in Chemistry,* vol. 3, p. 20, 2013.

[94] P. Zhang, D. Qiu, H. Chen, J. Sun, J. Wang, C. Qin*, et al.*, "Preparation of MWCNTs grafted with polyvinyl alcohol through Friedel–Crafts alkylation and their composite fibers with enhanced mechanical properties," *Journal of Materials Chemistry A,* vol. 3, pp. 1442-1449, 2015.

[95] J. Jyoti, S. Basu, B. P. Singh, and S. Dhakate, "Superior mechanical and electrical properties of multiwall carbon nanotube reinforced acrylonitrile butadiene styrene high performance composites," *Composites Part B: Engineering,* vol. 83, pp. 58-65, 2015.

[96] J. Gao, M. E. Itkis, A. Yu, E. Bekyarova, B. Zhao, and R. C. Haddon, "Continuous spinning of a single-walled carbon nanotube− nylon composite fiber," *Journal of the American Chemical Society,* vol. 127, pp. 3847-3854, 2005.

[97] J. Shin, C. Kim, and K. E. Geckeler, "Single-walled carbon nanotube–polystyrene nanocomposites: dispersing nanotubes in organic media," *Polymer International,* vol. 58, pp. 579-583, 2009.

[98] A. M. Esawi, H. G. Salem, H. M. Hussein, and A. R. Ramadan, "Effect of processing technique on the dispersion of carbon nanotubes within polypropylene carbon nanotube-composites and its effect on their mechanical properties," *Polymer composites,* vol. 31, pp. 772-780, 2010.

[99] J. Chen, B. Liu, X. Gao, and D. Xu, "A review of the interfacial characteristics of polymer nanocomposites containing carbon nanotubes," *RSC Advances,* vol. 8, pp. 28048-28085, 2018.

[100] T. Fornes, J. Baur, Y. Sabba, and E. Thomas, "Morphology and properties of melt-spun polycarbonate fibers containing single-and multi-wall carbon nanotubes," *Polymer,* vol. 47, pp. 1704-1714, 2006.

[101] M. Sennett, E. Welsh, J. Wright, W. Li, J. Wen, and Z. Ren, "Dispersion and alignment of carbon nanotubes in polycarbonate," *MRS Online Proceedings Library Archive,* vol. 706, 2001.

[102] J. Jang, J. Bae, and S.-H. Yoon, "A study on the effect of surface treatment of carbon nanotubes for liquid crystalline epoxide–carbon nanotube composites," *Journal of Materials Chemistry,* vol. 13, pp. 676-681, 2003.

[103] W. Feng, X. Bai, Y. Lian, J. Liang, X. Wang, and K. Yoshino, "Well-aligned polyaniline/carbon-nanotube composite films grown by in-situ aniline polymerization," *Carbon,* vol. 41, pp. 1551-1557, 2003.

[104] P. Ajayan, O. Stephan, C. Colliex, and D. Trauth, "Aligned carbon nanotube arrays formed by cutting a polymer resin—nanotube composite," *Science,* vol. 265, pp. 1212-1214, 1994.

[105] T. Kimura, H. Ago, M. Tobita, S. Ohshima, M. Kyotani, and M. Yumura, "Polymer composites of carbon nanotubes aligned by a magnetic field," *Advanced materials,* vol. 14, pp. 1380-1383, 2002.

[106] R. Sen, B. Zhao, D. Perea, M. E. Itkis, H. Hu, J. Love*, et al.*, "Preparation of single-walled carbon nanotube reinforced polystyrene and polyurethane nanofibers and membranes by electrospinning," *Nano letters,* vol. 4, pp. 459-464, 2004.

[107] M. D. Lynch and D. L. Patrick, "Organizing carbon nanotubes with liquid crystals," *Nano letters,* vol. 2, pp. 1197-1201, 2002.

[108] K. S. Khare, F. Khabaz, and R. Khare, "Effect of carbon nanotube functionalization on mechanical and thermal properties of cross-linked epoxy–carbon nanotube nanocomposites: role of strengthening the interfacial interactions," *ACS applied materials & interfaces,* vol. 6, pp. 6098-6110, 2014.

[109] C. Wang, J. Xu, J. Yang, Y. Qian, and H. Liu, "In-situ polymerization and multifunctional properties of surface-modified multiwalled carbon nanotube-reinforced polyimide nanocomposites," *High Performance Polymers,* vol. 29, pp. 797-807, 2017.

[110] Z.-K. Chen, J.-P. Yang, Q.-Q. Ni, S.-Y. Fu, and Y.-G. Huang, "Reinforcement of epoxy resins with multi-walled carbon nanotubes for enhancing cryogenic mechanical properties," *Polymer,* vol. 50, pp. 4753-4759, 2009.

[111] F. Gojny, M. Wichmann, U. Köpke, B. Fiedler, and K. Schulte, "Carbon nanotube-reinforced epoxy-composites: enhanced stiffness and fracture toughness at low nanotube content," *Composites science and technology,* vol. 64, pp. 2363-2371, 2004.

[112] R. Andrews and M. Weisenberger, "Carbon nanotube polymer composites," *Current Opinion in Solid State and Materials Science,* vol. 8, pp. 31-37, 2004.

[113] J. Cha, G. H. Jun, J. K. Park, J. C. Kim, H. J. Ryu, and S. H. Hong, "Improvement of modulus, strength and fracture toughness of CNT/Epoxy nanocomposites through the functionalization of carbon nanotubes," *Composites Part B: Engineering,* vol. 129, pp. 169-179, 2017.

[114] Y. Chen, B. Liu, X. He, Y. Huang, and K. Hwang, "Failure analysis and the optimal toughness design of carbon nanotube-reinforced composites," *Composites Science and Technology,* vol. 70, pp. 1360-1367, 2010.

[115] C. Ma, H.-Y. Liu, X. Du, L. Mach, F. Xu, and Y.-W. Mai, "Fracture resistance, thermal and electrical properties of epoxy composites containing aligned carbon nanotubes by low magnetic field," *Composites Science and Technology,* vol. 114, pp. 126-135, 2015.

[116] M. Ayatollahi, S. Shadlou, and M. Shokrieh, "Fracture toughness of epoxy/multi-walled carbon nanotube nano-composites under bending and shear loading conditions," *Materials & Design,* vol. 32, pp. 2115-2124, 2011.

[117] F. H. Gojny, M. H. Wichmann, B. Fiedler, and K. Schulte, "Influence of different carbon nanotubes on the mechanical properties of epoxy matrix composites–a comparative study," *Composites Science and Technology,* vol. 65, pp. 2300-2313, 2005.

[118] B. Coto, I. Antia, J. Barriga, M. Blanco, and J.-R. Sarasua, "Influence of the geometrical properties of the carbon nanotubes on the interfacial behavior of epoxy/CNT composites: a molecular modelling approach," *Computational Materials Science,* vol. 79, pp. 99-104, 2013.

[119] Y. J. Liu and X. Chen, "Evaluations of the effective material properties of carbon nanotube-based composites using a nanoscale representative volume element," *Mechanics of materials,* vol. 35, pp. 69-81, 2003.

[120] S.-G. Cho and K.-C. Ko, "Surface free energy and super-hydrophobic coating of multi-walled carbon nanotubes by 3: 1 TMCS/toluene glow discharge plasma under low pressure," *Thin solid films,* vol. 518, pp. 6619-6623, 2010.

[121] S. Nuriel, L. Liu, A. Barber, and H. Wagner, "Direct measurement of multiwall nanotube surface tension," *Chemical Physics Letters,* vol. 404, pp. 263-266, 2005.

[122] L. Zhang, J. Wang, C. A. Fuentes, D. Zhang, A. W. Van Vuure, J. W. Seo*, et al.*, "Wettability of carbon nanotube fibers," *Carbon,* vol. 122, pp. 128-140, 2017/10/01/ 2017.

[123] R. Atif and F. Inam, "Reasons and remedies for the agglomeration of multilayered graphene and carbon nanotubes in polymers," *Beilstein journal of nanotechnology,* vol. 7, p. 1174, 2016.

[124] C. He, N. Zhao, C. Shi, and S. Song, "Mechanical properties and microstructures of carbon nanotube-reinforced Al matrix composite fabricated by in situ chemical vapor deposition," *Journal of Alloys and Compounds,* vol. 487, pp. 258-262, 2009.

[125] K. Kondoh, T. Threrujirapapong, J. Umeda, and B. Fugetsu, "High-temperature properties of extruded titanium composites fabricated from carbon nanotubes coated titanium powder by spark plasma sintering and hot extrusion," *Composites science and technology,* vol. 72, pp. 1291-1297, 2012.

[126] H. Fukuda, K. Kondoh, J. Umeda, and B. Fugetsu, "Interfacial analysis between Mg matrix and carbon nanotubes in Mg–6 wt.% Al alloy matrix composites reinforced with carbon nanotubes," *Composites Science and Technology,* vol. 71, pp. 705-709, 2011.

[127] F. Ostovan, K. A. Matori, M. Toozandehjani, A. Oskoueian, H. M. Yusoff, R. Yunus*, et al.*, "Effects of CNTs content and milling time on mechanical behavior of MWCNT-reinforced aluminum nanocomposites," *Materials Chemistry and Physics,* vol. 166, pp. 160-166, 2015.

[128] S. Simões, F. Viana, M. A. Reis, and M. F. Vieira, "Influence of dispersion/mixture time on mechanical properties of Al–CNTs nanocomposites," *Composite Structures,* vol. 126, pp. 114-122, 2015.

[129] H. Kwon and M. Leparoux, "Hot extruded carbon nanotube reinforced aluminum matrix composite materials," *Nanotechnology,* vol. 23, p. 415701, 2012.

[130] J. Wu, H. Zhang, Y. Zhang, and X. Wang, "Mechanical and thermal properties of carbon nanotube/aluminum composites consolidated by spark plasma sintering," *Materials & Design,* vol. 41, pp. 344-348, 2012.

[131] J. Nguyen, H. Wen, Z. Zhang, F. Yaghmaie, and E. Lavernia, "Surfactant assisted dispersion and adhesion behavior of carbon nanotubes on Cu–Zr and Cu–Zr–Al amorphous powders," *Journal of Materials Science & Technology,* vol. 30, pp. 847-853, 2014.

[132] C. He, N. Zhao, C. Shi, X. Du, J. Li, H. Li*, et al.*, "An approach to obtaining homogeneously dispersed carbon nanotubes in Al Powders for preparing reinforced Al-matrix composites," *Advanced Materials,* vol. 19, pp. 1128-1132, 2007.

[133] M. H. Nai, J. Wei, and M. Gupta, "Interface tailoring to enhance mechanical properties of carbon nanotube reinforced magnesium composites," *Materials & Design,* vol. 60, pp. 490-495, 2014.

[134] Y. Park, K. Cho, I. Park, and Y. Park, "Fabrication and mechanical properties of magnesium matrix composite reinforced with Si coated carbon nanotubes," *Procedia Engineering,* vol. 10, pp. 1446-1450, 2011.

[135] H.-p. Li, J.-w. Fan, J.-l. Kang, N.-q. Zhao, X.-x. Wang, and B.-e. Li, "In-situ homogeneous synthesis of carbon nanotubes on aluminum matrix and properties of their composites," *Transactions of Nonferrous Metals Society of China,* vol. 24, pp. 2331-2336, 2014.

[136] K. T. Kim, S. I. Cha, S. H. Hong, and S. H. Hong, "Microstructures and tensile behavior of carbon nanotube reinforced Cu matrix nanocomposites," *Materials Science and Engineering: A,* vol. 430, pp. 27-33, 2006.

[137] W. M. Daoush, B. K. Lim, C. B. Mo, D. H. Nam, and S. H. Hong, "Electrical and mechanical properties of carbon nanotube reinforced copper nanocomposites fabricated by electroless deposition process," *Materials Science and Engineering: A,* vol. 513, pp. 247-253, 2009.

[138] A. M. Esawi and M. A. El Borady, "Carbon nanotube-reinforced aluminium strips," *Composites Science and Technology,* vol. 68, pp. 486-492, 2008.

[139] D. Chunfeng, X. ZHANG, M. Yanxia, and W. Dezun, "Fabrication of aluminum matrix composite reinforced with carbon nanotubes," *Rare Metals,* vol. 26, pp. 450-455, 2007.

[140] K. Vishwanath, G. Raji, A. Shakiba, and S. K. Murthy, "Mechanical properties of copper nanocomposites reinforced with uncoated and nickel coated carbon nanotubes," *FME Transactions,* vol. 46, pp. 623-630, 2018.

[141] C. Deng, Y. Ma, P. Zhang, X. Zhang, and D. Wang, "Thermal expansion behaviors of aluminum composite reinforced with carbon nanotubes," *Materials Letters,* vol. 62, pp. 2301-2303, 2008.

[142] C. Li, X. Wang, W. Liu, K. Wu, H. Shi, C. Ding*, et al.*, "Microstructure and strengthening mechanism of carbon nanotubes reinforced magnesium matrix composite," *Materials Science and Engineering: A,* vol. 597, pp. 264-269, 2014.

[143] T. Laha, Y. Chen, D. Lahiri, and A. Agarwal, "Tensile properties of carbon nanotube reinforced aluminum nanocomposite fabricated by plasma spray forming," *Composites Part A: Applied Science and Manufacturing,* vol. 40, pp. 589-594, 2009.

[144] F. Bonaccorso, L. Colombo, G. Yu, M. Stoller, V. Tozzini, A. C. Ferrari*, et al.*, "Graphene, related two-dimensional crystals, and hybrid systems for energy conversion and storage," *Science,* vol. 347, p. 1246501, 2015.

[145] C. Lee, X. Wei, J. W. Kysar, and J. Hone, "Measurement of the elastic properties and intrinsic strength of monolayer graphene," *science,* vol. 321, pp. 385-388, 2008.

[146] A. A. Balandin, "Thermal properties of graphene and nanostructured carbon materials," *Nature materials,* vol. 10, p. 569, 2011.

[147] J. R. Potts, D. R. Dreyer, C. W. Bielawski, and R. S. Ruoff, "Graphene-based polymer nanocomposites," *Polymer,* vol. 52, pp. 5-25, 2011.

[148] R. S. Edwards and K. S. Coleman, "Graphene synthesis: relationship to applications," *Nanoscale,* vol. 5, pp. 38-51, 2013.

[149] Y. Zhu, S. Murali, W. Cai, X. Li, J. W. Suk, J. R. Potts*, et al.*, "Graphene and graphene oxide: synthesis, properties, and applications," *Advanced materials,* vol. 22, pp. 3906-3924, 2010.

[150] K. S. Novoselov, V. Fal, L. Colombo, P. Gellert, M. Schwab, and K. Kim, "A roadmap for graphene," *nature,* vol. 490, p. 192, 2012.

[151] Y. Zhang, J. E. Mark, Y. Zhu, R. S. Ruoff, and D. W. Schaefer, "Mechanical properties of

polybutadiene reinforced with octadecylamine modified graphene oxide," *Polymer,* vol. 55, pp. 5389-5395, 2014.

[152] S. Wu, R. B. Ladani, J. Zhang, E. Bafekrpour, K. Ghorbani, A. P. Mouritz*, et al.*, "Aligning multilayer graphene flakes with an external electric field to improve multifunctional properties of epoxy nanocomposites," *Carbon,* vol. 94, pp. 607-618, 2015.

[153] Z. Li, J. Chu, C. Yang, S. Hao, M. A. Bissett, I. A. Kinloch*, et al.*, "Effect of functional groups on the agglomeration of graphene in nanocomposites," *Composites Science and Technology,* vol. 163, pp. 116-122, 2018.

[154] H. Kim and C. W. Macosko, "Processing-property relationships of polycarbonate/graphene composites," *Polymer,* vol. 50, pp. 3797-3809, 2009.

[155] H. Kim and C. W. Macosko, "Morphology and properties of polyester/exfoliated graphite nanocomposites," *Macromolecules,* vol. 41, pp. 3317-3327, 2008.

[156] K. Wakabayashi, C. Pierre, D. A. Dikin, R. S. Ruoff, T. Ramanathan, L. C. Brinson*, et al.*, "Polymer–Graphite Nanocomposites: Effective Dispersion and Major Property Enhancement via Solid-State Shear Pulverization," *Macromolecules,* vol. 41, pp. 1905-1908, 2008.

[157] M. Klüppel, "The role of disorder in filler reinforcement of elastomers on various length scales," in *Filler-Reinforced Elastomers/Sanning Force Microscopy*, ed: Springer, 2003, pp. 1-86.

[158] D. Paul and L. M. Robeson, "Polymer nanotechnology: nanocomposites," *Polymer,* vol. 49, pp. 3187-3204, 2008.

[159] L. Schadler, S. a. Giannaris, and P. Ajayan, "Load transfer in carbon nanotube epoxy composites," *Applied physics letters,* vol. 73, pp. 3842-3844, 1998.

[160] M. A. Rafiee, J. Rafiee, I. Srivastava, Z. Wang, H. Song, Z. Z. Yu*, et al.*, "Fracture and fatigue in graphene nanocomposites," *small,* vol. 6, pp. 179-183, 2010.

[161] P. Pötschke, M. Abdel-Goad*, S. Pegel, D. Jehnichen, J. E. Mark, D. Zhou***, et al.*, "Comparisons among electrical and rheological properties of melt-mixed composites containing various carbon nanostructures," *Journal of Macromolecular Science, Part A,* vol. 47, pp. 12-19, 2009.

[162] X. Zhao, Q. Zhang, D. Chen, and P. Lu, "Enhanced mechanical properties of graphene-based poly (vinyl alcohol) composites," *Macromolecules,* vol. 43, pp. 2357-2363, 2010.

[163] I. Zaman, T. T. Phan, H.-C. Kuan, Q. Meng, L. T. B. La, L. Luong*, et al.*, "Epoxy/graphene platelets nanocomposites with two levels of interface strength," *Polymer,* vol. 52, pp. 1603-1611, 2011.

[164] F. Piana and J. Pionteck, "Effect of the melt processing conditions on the conductive paths formation in thermoplastic polyurethane/expanded graphite (TPU/EG) composites," *Composites Science and Technology,* vol. 80, pp. 39-46, 2013.

[165] N. Domun, H. Hadavinia, T. Zhang, T. Sainsbury, G. Liaghat, and S. Vahid, "Improving the fracture toughness and the strength of epoxy using nanomaterials–a review of the current status," *Nanoscale,* vol. 7, pp. 10294-10329, 2015.

[166] M. A. Rafiee, W. Lu, A. V. Thomas, A. Zandiatashbar, J. Rafiee, J. M. Tour*, et al.*, "Graphene nanoribbon composites," *ACS nano,* vol. 4, pp. 7415-7420, 2010.

[167] J. Wang, Z. Li, G. Fan, H. Pan, Z. Chen, and D. Zhang, "Reinforcement with graphene nanosheets in aluminum matrix composites," *Scripta Materialia,* vol. 66, pp. 594-597, 2012.

[168] R. Pérez-Bustamante, D. Bolaños-Morales, J. Bonilla-Martínez, I. Estrada-Guel, and R. Martínez-Sánchez, "Microstructural and hardness behavior of graphene-nanoplatelets/aluminum composites synthesized by mechanical alloying," *Journal of Alloys and Compounds,* vol. 615, pp. S578-S582, 2014.

[169] C. YANG, "Research of graphene-reinforced aluminum matrix nanocomposites," *Journal of Materials Engineering,* vol. 1, pp. 1-6, 2011.

[170] P. Ashwath and M. A. Xavior, "The effect of ball milling & reinforcement percentage on sintered samples of aluminium alloy metal matrix composites," *Procedia Engineering,* vol. 97, pp. 1027-1032, 2014.

[171] S. F. Bartolucci, J. Paras, M. A. Rafiee, J. Rafiee, S. Lee, D. Kapoor*, et al.*, "Graphene–aluminum nanocomposites," *Materials Science and Engineering: A,* vol. 528, pp. 7933-7937, 2011.

[172] Z. Li, G. Fan, Z. Tan, Q. Guo, D. Xiong, Y. Su*, et al.*, "Uniform dispersion of graphene oxide in aluminum powder by direct electrostatic adsorption for fabrication of graphene/aluminum composites," *Nanotechnology,* vol. 25, p. 325601, 2014.

[173] M. Rashad, F. Pan, A. Tang, M. Asif, J. She, J. Gou*, et al.*, "Development of magnesium-graphene nanoplatelets composite," *Journal of composite materials,* vol. 49, pp. 285-293, 2015.

[174] D. Kuang, L. Xu, L. Liu, W. Hu, and Y. Wu, "Graphene–nickel composites," *Applied Surface*

Science, vol. 273, pp. 484-490, 2013.

[175] W. Zhai, X. Shi, J. Yao, A. M. M. Ibrahim, Z. Xu, Q. Zhu*, et al.*, "Investigation of mechanical and tribological behaviors of multilayer graphene reinforced Ni3Al matrix composites," *Composites Part B: Engineering,* vol. 70, pp. 149-155, 2015.

[176] R. Arsenault and N. Shi, "Dislocation generation due to differences between the coefficients of thermal expansion," *Materials Science and Engineering,* vol. 81, pp. 175-187, 1986.

[177] M. Rashad, F. Pan, and M. Asif, "Magnesium matrix composites reinforced with graphene nanoplatelets," *Graphene Materials: Fundamentals and Emerging Applications,* pp. 151-189, 2015.

[178] C. P. Kumar, T. Venkatesha, and R. Shabadi, "Preparation and corrosion behavior of Ni and Ni–graphene composite coatings," *Materials Research Bulletin,* vol. 48, pp. 1477-1483, 2013.

[179] Z. Ren, N. Meng, K. Shehzad, Y. Xu, S. Qu, B. Yu*, et al.*, "Mechanical properties of nickel-graphene composites synthesized by electrochemical deposition," *Nanotechnology,* vol. 26, p. 065706, 2015.

[180] D. Lin, C. R. Liu, and G. J. Cheng, "Single-layer graphene oxide reinforced metal matrix composites by laser sintering: Microstructure and mechanical property enhancement," *Acta materialia,* vol. 80, pp. 183-193, 2014.

[181] M. Bastwros, G.-Y. Kim, K. Zhang, and S. Wang, "Fabrication of graphene reinforced aluminum composite by semi-solid processing," in *ASME 2013 International Mechanical Engineering Congress and Exposition*, 2013, pp. V02BT02A030-V02BT02A030.

[182] Y. Song, W. Liu, and Y. Chen, "Strengthening in a copper composite containing graphene nanofillers," in *IOP Conference Series: Materials Science and Engineering*, 2017, p. 012017.

[183] L.-Y. Chen, H. Konishi, A. Fehrenbacher, C. Ma, J.-Q. Xu, H. Choi*, et al.*, "Novel nanoprocessing route for bulk graphene nanoplatelets reinforced metal matrix nanocomposites," *Scripta Materialia,* vol. 67, pp. 29-32, 2012.

[184] J. Hwang, T. Yoon, S. H. Jin, J. Lee, T. S. Kim, S. H. Hong*, et al.*, "Enhanced mechanical properties of graphene/copper nanocomposites using a molecular-level mixing process," *Advanced materials,* vol. 25, pp. 6724-6729, 2013.

[185] Y. Tang, X. Yang, R. Wang, and M. Li, "Enhancement of the mechanical properties of graphene–copper composites with graphene–nickel hybrids," *Materials Science and Engineering: A,* vol. 599, pp. 247-254, 2014.

[186] B. Lim, C.-j. Kim, B. Kim, U. Shim, S. Oh, B.-h. Sung*, et al.*, "The effects of interfacial bonding on mechanical properties of single-walled carbon nanotube reinforced copper matrix nanocomposites," *Nanotechnology,* vol. 17, p. 5759, 2006.

[187] Z. Xu and M. J. Buehler, "Interface structure and mechanics between graphene and metal substrates: a first-principles study," *Journal of Physics: Condensed Matter,* vol. 22, p. 485301, 2010.

[188] M. Rashad, F. Pan, A. Tang, Y. Lu, M. Asif, S. Hussain*, et al.*, "Effect of graphene nanoplatelets (GNPs) addition on strength and ductility of magnesium-titanium alloys," *Journal of Magnesium and alloys,* vol. 1, pp. 242-248, 2013.

[189] E. P. Giannelis, "A new strategy for synthesizing polymer-ceramic nanocomposites," *Jom,* vol. 44, pp. 28-30, 1992.

[190] Y. Kojima, A. Usuki, M. Kawasumi, A. Okada, T. Kurauchi, and O. Kamigaito, "Sorption of water in nylon 6-clay hybrid," *Journal of applied polymer science,* vol. 49, pp. 1259-1264, 1993.

[191] R. A. Vaia, H. Ishii, and E. P. Giannelis, "Synthesis and properties of two-dimensional nanostructures by direct intercalation of polymer melts in layered silicates," *Chemistry of materials,* vol. 5, pp. 1694-1696, 1993.

[192] P. B. Messersmith and E. P. Giannelis, "Synthesis and characterization of layered silicate-epoxy nanocomposites," *Chemistry of materials,* vol. 6, pp. 1719-1725, 1994.

[193] L. Biasci, M. Aglietto, G. Ruggeri, and F. Ciardelli, "Functionalization of montmorillonite by methyl methacrylate polymers containing side-chain ammonium cations," *Polymer,* vol. 35, pp. 3296-3304, 1994.

[194] G. Jimenez, N. Ogata, H. Kawai, and T. Ogihara, "Structure and thermal/mechanical properties of poly (ϵ-caprolactone)-clay blend," *Journal of Applied Polymer Science,* vol. 64, pp. 2211-2220, 1997.

[195] Y. Kurokawa, H. Yasuda, M. Kashiwagi, and A. Oyo, "Structure and properties of a montmorillonite/polypropylene nanocomposite," *Journal of materials science letters,* vol. 16,

pp. 1670-1672, 1997.

[196] Z. Wang and T. J. Pinnavaia, "Nanolayer reinforcement of elastomeric polyurethane," *Chemistry of Materials,* vol. 10, pp. 3769-3771, 1998.

[197] Z. K. Zhu, Y. Yang, J. Yin, X. Y. Wang, Y. C. Ke, and Z. N. Qi, "Preparation and properties of organosoluble montmorillonite/polyimide hybrid materials," *Journal of applied polymer science,* vol. 73, pp. 2063-2068, 1999.

[198] V. Agubra, P. Owuor, and M. Hosur, "Influence of nanoclay dispersion methods on the mechanical behavior of E-glass/epoxy nanocomposites," *Nanomaterials,* vol. 3, pp. 550-563, 2013.

[199] R. N. Choi, C. I. Cheigh, S. Y. Lee, and M. S. Chung, "Preparation and properties of polypropylene/clay nanocomposites for food packaging," *Journal of food science,* vol. 76, pp. N62-N67, 2011.

[200] L. Wang, K. Wang, L. Chen, Y. Zhang, and C. He, "Preparation, morphology and thermal/mechanical properties of epoxy/nanoclay composite," *Composites Part A: applied science and manufacturing,* vol. 37, pp. 1890-1896, 2006.

[201] S. Peeterbroeck, M. Alexandre, R. Jérôme, and P. Dubois, "Poly (ethylene-co-vinyl acetate)/clay nanocomposites: Effect of clay nature and organic modifiers on morphology, mechanical and thermal properties," *Polymer degradation and stability,* vol. 90, pp. 288-294, 2005.

[202] S. Abbasi, P. J. Carreau, A. Derdouri, and M. Moan, "Rheological properties and percolation in suspensions of multiwalled carbon nanotubes in polycarbonate," *Rheologica acta,* vol. 48, p. 943, 2009.

[203] M.-J. Khalaj, H. Ahmadi, R. Lesankhosh, and G. Khalaj, "Study of physical and mechanical properties of polypropylene nanocomposites for food packaging application: Nano-clay modified with iron nanoparticles," *Trends in Food Science & Technology,* vol. 51, pp. 41-48, 2016.

[204] T. Fornes, P. Yoon, H. Keskkula, and D. Paul, "Nylon 6 nanocomposites: the effect of matrix molecular weight," *Polymer,* vol. 42, pp. 09929-09940, 2001.

[205] B. Finnigan, D. Martin, P. Halley, R. Truss, and K. Campbell, "Morphology and properties of thermoplastic polyurethane nanocomposites incorporating hydrophilic layered silicates," *Polymer,* vol. 45, pp. 2249-2260, 2004.

[206] M. Zamanian, M. Mortezaei, B. Salehnia, and J. Jam, "Fracture toughness of epoxy polymer modified with nanosilica particles: Particle size effect," *Engineering Fracture Mechanics,* vol. 97, pp. 193-206, 2013.

[207] B. Johnsen, A. Kinloch, R. Mohammed, A. Taylor, and S. Sprenger, "Toughening mechanisms of nanoparticle-modified epoxy polymers," *Polymer,* vol. 48, pp. 530-541, 2007.

[208] N. Eustathopoulos, M. G. Nicholas, and B. Drevet, *Wettability at high temperatures* vol. 3: Elsevier, 1999.

[209] R. Aikin, "The mechanical properties of in-situ composites," *JOM,* vol. 49, p. 35, 1997.

[210] Y.-T. Zhao, S.-L. Zhang, G. Chen, X.-N. Cheng, and C.-Q. Wang, "In situ (Al2O3+ Al3Zr) np/Al nanocomposites synthesized by magneto-chemical melt reaction," *Composites Science and Technology,* vol. 68, pp. 1463-1470, 2008.

[211] D. Stinton, T. Besmann, and R. Lowden, "Advanced ceramics by chemical vapor deposition techniques," *American ceramic society bulletin,* vol. 67, pp. 350-355, 1988.

[212] S. Tjong and H. Chen, "Nanocrystalline materials and coatings," *Materials Science and Engineering: R: Reports,* vol. 45, pp. 1-88, 2004.

[213] R. Alexandrescu, E. Borsella, S. Botti, M. Cesile, S. Martelli, R. Giorgi*, et al.*, "Synthesis of TiC and SiC/TiC nanocrystalline powders by gas-phase laser-induced reaction," *Journal of materials science,* vol. 32, pp. 5629-5635, 1997.

[214] D. K. Koli, G. Agnihotri, and R. Purohit, "Properties and characterization of Al-Al2O3 composites processed by casting and powder metallurgy routes," *International Journal of Latest Trends in Engineering and Technology (IJLTET),* vol. 2, pp. 486-496, 2013.

[215] S. A. Sajjadi and S. M. Zebarjad, "Synthesis of Al-Al2O3 nano-composite by mechanical alloying and evaluation of the effect of ball milling time on the microstructure and mechanical properties," in *ICMN08*, 2008.

[216] X. Zeng, W. Liu, B. Xu, G. Shu, and Q. Li, "Microstructure and Mechanical Properties of Al–SiC Nanocomposites Synthesized by Surface-Modified Aluminium Powder," *Metals,* vol. 8, p. 253, 2018.

[217] Y.-C. Kang and S. L.-I. Chan, "Tensile properties of nanometric Al2O3 particulate-reinforced aluminum matrix composites," *Materials chemistry and physics,* vol. 85, pp. 438-443, 2004.

[218] D. Jia, "Influence of SiC particulate size on the microstructural evolution and mechanical properties of Al–6Ti–6Nb matrix composites," *Materials Science and Engineering: A,* vol. 289, pp. 83-90, 2000.

[219] F. Tang, M. Hagiwara, and J. M. Schoenung, "Microstructure and tensile properties of bulk nanostructured Al-5083/SiCp composites prepared by cryomilling," *Materials Science and Engineering: A,* vol. 407, pp. 306-314, 2005.

[220] C. Hsu, C. Chang, P. Kao, N. Ho, and C. Chang, "Al–Al3Ti nanocomposites produced in situ by friction stir processing," *Acta Materialia,* vol. 54, pp. 5241-5249, 2006.

[221] R. Rai, S. Saha, G. Datta, and M. Chakraborty, "Studies on synthesis of in-situ Al-TiC metal matrix composites," in *IOP Conference Series: Materials Science and Engineering*, 2016, p. 012042.

[222] L. Poovazhagan, K. Kalaichelvan, and A. Rajadurai, "Preparation of SiC nano-particulates reinforced aluminum matrix nanocomposites by high intensity ultrasonic cavitation process," *Transactions of the Indian Institute of Metals,* vol. 67, pp. 229-237, 2014.

[223] W. E Wong and M. Gupta, "Simultaneously improving strength and ductility of magnesium using nano-size SiC particulates and microwaves," *Advanced Engineering Materials,* vol. 8, pp. 735-740, 2006.

[224] G. Cao, J. Kobliska, H. Konishi, and X. Li, "Tensile properties and microstructure of SiC nanoparticle–reinforced Mg-4Zn alloy fabricated by ultrasonic cavitation–based solidification processing," *Metallurgical and Materials Transactions A,* vol. 39, pp. 880-886, 2008.

[225] H. Ferkel and B. Mordike, "Magnesium strengthened by SiC nanoparticles," *Materials Science and Engineering: A,* vol. 298, pp. 193-199, 2001.

[226] M. Vanarotti, S. Kori, B. Sridhar, and S. B. Padasalgi, "Synthesis and characterization of aluminium alloy A356 and silicon carbide metal matrix composite," in *International Conference on Industrial Technology and Management*, 2012, pp. 11-15.

[227] M. M. Boopathi, K. Arulshri, and N. Iyandurai, "Evaluation of mechanical properties of aluminium alloy 2024 reinforced with silicon carbide and fly ash hybrid metal matrix composites," *American journal of applied sciences,* vol. 10, p. 219, 2013.

[228] Y. Yang, J. Lan, and X. Li, "Study on bulk aluminum matrix nano-composite fabricated by ultrasonic dispersion of nano-sized SiC particles in molten aluminum alloy," *Materials Science and Engineering: A,* vol. 380, pp. 378-383, 2004.

[229] S. Jiguet, M. Judelewicz, S. Mischler, A. Bertch, and P. Renaud, "Effect of filler behavior on nanocomposite SU8 photoresist for moving micro-parts," *Microelectronic engineering,* vol. 83, pp. 1273-1276, 2006.

[230] R. Kitey and H. Tippur, "Role of particle size and filler–matrix adhesion on dynamic fracture of glass-filled epoxy. I. Macromeasurements," *Acta Materialia,* vol. 53, pp. 1153-1165, 2005.

[231] J. Douce, J.-P. Boilot, J. Biteau, L. Scodellaro, and A. Jimenez, "Effect of filler size and surface condition of nano-sized silica particles in polysiloxane coatings," *Thin Solid Films,* vol. 466, pp. 114-122, 2004.

[232] S. Mishra, S. Sonawane, and R. Singh, "Studies on characterization of nano CaCO3 prepared by the in situ deposition technique and its application in PP-nano CaCO3 composites," *Journal of Polymer Science Part B: Polymer Physics,* vol. 43, pp. 107-113, 2005.

[233] J. C. Kearns and R. L. Shambaugh, "Polypropylene fibers reinforced with carbon nanotubes," *Journal of Applied Polymer Science,* vol. 86, pp. 2079-2084, 2002.

[234] X. Chen, J. Wang, M. Lin, W. Zhong, T. Feng, X. Chen*, et al.*, "Mechanical and thermal properties of epoxy nanocomposites reinforced with amino-functionalized multi-walled carbon nanotubes," *Materials Science and Engineering: A,* vol. 492, pp. 236-242, 2008.

[235] H. G. Chae, M. L. Minus, and S. Kumar, "Oriented and exfoliated single wall carbon nanotubes in polyacrylonitrile," *Polymer,* vol. 47, pp. 3494-3504, 2006.

[236] J. Vacha and M. Boruka, "Mechanical Properties of Acrylonitrile Butadiene Styrene Thermoplastic Polymer Matrix with Carbon Nanotubes," ed: NANOCON, 2015.

[237] S. U. Khan, J. R. Pothnis, and J.-K. Kim, "Effects of carbon nanotube alignment on electrical and mechanical properties of epoxy nanocomposites," *Composites Part A: Applied Science and Manufacturing,* vol. 49, pp. 26-34, 2013.

[238] S. Jangam, S. Raja, and K. H. Reddy, "Effect of multiwalled carbon nanotube alignment on the tensile fatigue behavior of nanocomposites," *Journal of Composite Materials,* vol. 52, pp. 2365-

2374, 2018.
[239] J. Shiju, F. Al-Sagheer, A. Bumajdad, and Z. Ahmad, "In-Situ Preparation of Aramid-Multiwalled CNT Nano-Composites: Morphology, Thermal Mechanical and Electric Properties," *Nanomaterials,* vol. 8, p. 309, 2018.
[240] F. Buffa, G. A. Abraham, B. P. Grady, and D. Resasco, "Effect of nanotube functionalization on the properties of single-walled carbon nanotube/polyurethane composites," *Journal of Polymer Science Part B: Polymer Physics,* vol. 45, pp. 490-501, 2007.
[241] W. Leininger, X. Wang, and X. Tangpong, "Effects of MWCNT reinforcement on quasi-static and dynamic tensile properties of epoxy," *Journal of Composite Materials,* vol. 48, pp. 2049-2057, 2014.
[242] N. Hong, J. Zhan, X. Wang, A. A. Stec, T. R. Hull, H. Ge*, et al.*, "Enhanced mechanical, thermal and flame retardant properties by combining graphene nanosheets and metal hydroxide nanorods for Acrylonitrile–Butadiene–Styrene copolymer composite," *Composites Part A: Applied Science and Manufacturing,* vol. 64, pp. 203-210, 2014.
[243] J. R. Potts, S. H. Lee, T. M. Alam, J. An, M. D. Stoller, R. D. Piner*, et al.*, "Thermomechanical properties of chemically modified graphene/poly (methyl methacrylate) composites made by in situ polymerization," *Carbon,* vol. 49, pp. 2615-2623, 2011.
[244] Z. Li, R. Wang, R. J. Young, L. Deng, F. Yang, L. Hao*, et al.*, "Control of the functionality of graphene oxide for its application in epoxy nanocomposites," *Polymer,* vol. 54, pp. 6437-6446, 2013.
[245] J. i. Masuda and J. M. Torkelson, "Dispersion and major property enhancements in polymer/multiwall carbon nanotube nanocomposites via solid-state shear pulverization followed by melt mixing," *Macromolecules,* vol. 41, pp. 5974-5977, 2008.
[246] J. Roul, S. K. Sahoo, and R. Mohapatra, "Design and characterization of biodegradable polymer-clay nanocomposites prepared by solution mixing technique," *International Journal of Nano Dimension,* vol. 4, pp. 135-139, 2013.
[247] Q. Zeng, D. Wang, A. Yu, and G. Lu, "Synthesis of polymer–montmorillonite nanocomposites by in situ intercalative polymerization," *Nanotechnology,* vol. 13, p. 549, 2002.
[248] M. Lee, B. Kim, J. Nam, Y. Lee, Y. Son, and S. Seo, "In-situ formation of gold nanoparticle/conducting polymer nanocomposites," *Molecular Crystals and Liquid Crystals,* vol. 407, pp. 1-6, 2003.
[249] I. A. Rahman and V. Padavettan, "Synthesis of silica nanoparticles by sol-gel: size-dependent properties, surface modification, and applications in silica-polymer nanocomposites—a review," *Journal of Nanomaterials,* vol. 2012, p. 8, 2012.
[250] Y.-H. Choa, J.-K. Yang, B.-H. Kim, Y.-K. Jeong, J.-S. Lee, T. Nakayama*, et al.*, "Preparation and characterization of metal/ceramic nanoporous nanocomposite powders," *Journal of Magnetism and Magnetic Materials,* vol. 266, pp. 12-19, 2003.
[251] S.-m. Zhou, X.-b. Zhang, Z.-p. Ding, C.-y. Min, G.-l. Xu, and W.-m. Zhu, "Fabrication and tribological properties of carbon nanotubes reinforced Al composites prepared by pressureless infiltration technique," *Composites Part A: Applied Science and Manufacturing,* vol. 38, pp. 301-306, 2007.
[252] X. Li, Y. Yang, and X. Cheng, "Ultrasonic-assisted fabrication of metal matrix nanocomposites," *Journal of Materials Science,* vol. 39, pp. 3211-3212, 2004.
[253] D. Ying and D. Zhang, "Processing of Cu–Al2O3 metal matrix nanocomposite materials by using high energy ball milling," *Materials Science and Engineering: A,* vol. 286, pp. 152-156, 2000.
[254] Y. Cao, Q. Su, R. Che, G. Du, and B. Xu, "One-step chemical vapor synthesis of Ni/graphene nanocomposites with excellent electromagnetic and electrocatalytic properties," *Synthetic Metals,* vol. 162, pp. 968-973, 2012.
[255] M. Joseph, C. Tsotsos, M. Baker, P. Kench, C. Rebholz, A. Matthews*, et al.*, "Characterisation and tribological evaluation of nitrogen-containing molybdenum–copper PVD metallic nanocomposite films," *Surface and Coatings Technology,* vol. 190, pp. 345-356, 2005.
[256] P. V. Kamat, M. Flumiani, and A. Dawson, "Metal–metal and metal–semiconductor composite nanoclusters," *Colloids and Surfaces A: Physicochemical and Engineering Aspects,* vol. 202, pp. 269-279, 2002.
[257] S. Roy, D. Das, D. Chakravorty, and D. Agrawal, "Magnetic properties of glass-metal nanocomposites prepared by the sol-gel route and hot pressing," *Journal of applied physics,* vol. 74, pp. 4746-4749, 1993.

[258] Y. Choa, S. Yoo, J. Yang, J. Park, S. Oh, K. Kang*, et al.*, "PART 2-C-05 Ceramic Materials-Effect of Powder Synthesis Processing on the Microstructure and Electrical Conductivity of Sintered CNTs/Fe/Al2O3 Nanocomposites," in *Materials Science Forum*, 2007, p. 1021.

[259] W. R. Schmidt, D. M. Narsavage-Heald, D. M. Jones, P. S. Marchetti, D. Raker, and G. E. Maciel, "Poly (borosilazane) precursors to ceramic nanocomposites," *Chemistry of materials,* vol. 11, pp. 1455-1464, 1999.

[260] G. Ennas, A. Mei, A. Musinu, G. Piccaluga, G. Pinna, and S. Solinas, "Sol–gel preparation and characterization of Ni–SiO2 nanocomposites," *Journal of non-crystalline solids,* vol. 232, pp. 587-593, 1998.

[261] Z. Baig, O. Mamat, M. Mustapha, A. Mumtaz, M. Sarfraz, and S. Haider, "An efficient approach to address issues of graphene nanoplatelets (GNPs) incorporation in aluminium powders and their compaction behaviour," *Metals,* vol. 8, p. 90, 2018.

[262] C. T. Kingston, Z. J. Jakubek, S. Dénommée, and B. Simard, "Efficient laser synthesis of single-walled carbon nanotubes through laser heating of the condensing vaporization plume," *Carbon,* vol. 42, pp. 1657-1664, 2004.

[263] H. Gustafsson, S. Isaksson, A. Altskär, and K. Holmberg, "Mesoporous silica nanoparticles with controllable morphology prepared from oil-in-water emulsions," *Journal of colloid and interface science,* vol. 467, pp. 253-260, 2016.

[264] M. Ayatollahi, S. Shadlou, M. Shokrieh, and M. Chitsazzadeh, "Effect of multi-walled carbon nanotube aspect ratio on mechanical and electrical properties of epoxy-based nanocomposites," *Polymer Testing,* vol. 30, pp. 548-556, 2011.

[265] F. Inam, T. Vo, J. P. Jones, and X. Lee, "Effect of carbon nanotube lengths on the mechanical properties of epoxy resin: An experimental study," *Journal of Composite Materials,* vol. 47, pp. 2321-2330, 2013.

[266] R. Hollertz, S. Chatterjee, H. Gutmann, T. Geiger, F. Nüesch, and B. Chu, "Improvement of toughness and electrical properties of epoxy composites with carbon nanotubes prepared by industrially relevant processes," *Nanotechnology,* vol. 22, p. 125702, 2011.

[267] S. R. Bakshi, V. Singh, S. Seal, and A. Agarwal, "Aluminum composite reinforced with multiwalled carbon nanotubes from plasma spraying of spray dried powders," *Surface and Coatings Technology,* vol. 203, pp. 1544-1554, 2009.

[268] J. Tu, Y. Yang, L. Wang, X. Ma, and X. Zhang, "Tribological properties of carbon-nanotube-reinforced copper composites," *Tribology Letters,* vol. 10, pp. 225-228, 2001.

[269] H. Deng, J. Yi, C. Xia, and Y. Yi, "Mechanical properties and microstructure characterization of well-dispersed carbon nanotubes reinforced copper matrix composites," *Journal of Alloys and Compounds,* vol. 727, pp. 260-268, 2017.

[270] G.-R. Shen, Y.-T. Cheng, and L.-N. Tsai, "Synthesis and characterization of Ni-P-CNT's nanocomposite film for MEMS applications," *IEEE Transactions on Nanotechnology,* vol. 4, pp. 539-547, 2005.

[271] J. Nguyen, T. B. Holland, H. Wen, M. Fraga, A. Mukherjee, and E. Lavernia, "Mechanical behavior of ultrafine-grained Ni–carbon nanotube composite," *Journal of materials science,* vol. 49, pp. 2070-2077, 2014.

[272] C. Goh, J. Wei, L. Lee, and M. Gupta, "Simultaneous enhancement in strength and ductility by reinforcing magnesium with carbon nanotubes," *Materials Science and Engineering: A,* vol. 423, pp. 153-156, 2006.

[273] M. Zhou, X. Qu, L. Ren, L. Fan, Y. Zhang, Y. Guo*, et al.*, "The effects of carbon nanotubes on the mechanical and wear properties of AZ31 alloy," *Materials,* vol. 10, p. 1385, 2017.

[274] J. Wei, R. Atif, T. Vo, and F. Inam, "Graphene nanoplatelets in epoxy system: dispersion, reaggregation, and mechanical properties of nanocomposites," *Journal of Nanomaterials,* vol. 16, p. 374, 2015.

[275] C. Salom, M. Prolongo, A. Toribio, A. Martínez-Martínez, I. A. de Cárcer, and S. Prolongo, "Mechanical properties and adhesive behavior of epoxy-graphene nanocomposites," *International Journal of Adhesion and Adhesives,* vol. 84, pp. 119-125, 2018.

[276] C. E. Corcione, F. Freuli, and A. Maffezzoli, "The aspect ratio of epoxy matrix nanocomposites reinforced with graphene stacks," *Polymer Engineering & Science,* vol. 53, pp. 531-539, 2013.

[277] L.-C. Tang, Y.-J. Wan, D. Yan, Y.-B. Pei, L. Zhao, Y.-B. Li*, et al.*, "The effect of graphene dispersion on the mechanical properties of graphene/epoxy composites," *Carbon,* vol. 60, pp. 16-27, 2013.

[278] M. A. Rafiee, J. Rafiee, Z. Wang, H. Song, Z.-Z. Yu, and N. Koratkar, "Enhanced mechanical properties of nanocomposites at low graphene content," *ACS nano,* vol. 3, pp. 3884-3890, 2009.

[279] J. Wei and F. Inam, "Processing of epoxy/graphene nanocomposites: Effects of surfactants," *Journal of Polymer Science & Applications,* vol. 1, p. 1000101, 2017.

[280] E. Lago, P. S. Toth, G. Pugliese, V. Pellegrini, and F. Bonaccorso, "Solution blending preparation of polycarbonate/graphene composite: boosting the mechanical and electrical properties," *RSC Advances,* vol. 6, pp. 97931-97940, 2016.

[281] M. El Achaby and A. Qaiss, "Processing and properties of polyethylene reinforced by graphene nanosheets and carbon nanotubes," *Materials & Design,* vol. 44, pp. 81-89, 2013.

[282] H. Kim, S. Kobayashi, M. A. AbdurRahim, M. J. Zhang, A. Khusainova, M. A. Hillmyer*, et al.*, "Graphene/polyethylene nanocomposites: effect of polyethylene functionalization and blending methods," *Polymer,* vol. 52, pp. 1837-1846, 2011.

[283] S. J. Yan, C. Yang, Q. H. Hong, J.-z. Chen, D. B. Liu, and S. L. Dai, *Research of graphene-reinforced aluminum matrix nanocomposites*, 2014.

[284] C.-H. Jeon, Y.-H. Jeong, J.-J. Seo, H. N. Tien, S.-T. Hong, Y.-J. Yum*, et al.*, "Material properties of graphene/aluminum metal matrix composites fabricated by friction stir processing," *International Journal of Precision Engineering and Manufacturing,* vol. 15, pp. 1235-1239, June 01 2014.

[285] J. Li, Y. Xiong, X. Wang, S. Yan, C. Yang, W. He*, et al.*, "Microstructure and tensile properties of bulk nanostructured aluminum/graphene composites prepared via cryomilling," *Materials Science and Engineering: A,* vol. 626, pp. 400-405, 2015.

[286] T. S. Koltsova, L. I. Nasibulina, I. V. Anoshkin, V. V. Mishin, E. I. Kauppinen, O. V. Tolochko*, et al.*, "New hybrid copper composite materials based on carbon nanostructures," *Journal of Materials Science and Engineering B,* vol. 2, pp. 240-246, 2012.

[287] C. L. Pavithra, B. V. Sarada, K. V. Rajulapati, T. N. Rao, and G. Sundararajan, "A new electrochemical approach for the synthesis of copper-graphene nanocomposite foils with high hardness," *Scientific reports,* vol. 4, p. 4049, 2014.

[288] M. Li, H. Che, X. Liu, S. Liang, and H. Xie, "Highly enhanced mechanical properties in Cu matrix composites reinforced with graphene decorated metallic nanoparticles," *Journal of materials science,* vol. 49, pp. 3725-3731, 2014.

[289] D.-B. Xiong, M. Cao, Q. Guo, Z. Tan, G. Fan, Z. Li*, et al.*, "Graphene-and-copper artificial nacre fabricated by a preform impregnation process: bioinspired strategy for strengthening-toughening of metal matrix composite," *Acs Nano,* vol. 9, pp. 6934-6943, 2015.

[290] C. Zhao and J. Wang, "Fabrication and tensile properties of graphene/copper composites prepared by electroless plating for structrual applications," *physica status solidi (a),* vol. 211, pp. 2878-2885, 2014.

[291] M. Rashad, F. Pan, M. Asif, and A. Tang, "Powder metallurgy of Mg–1% Al–1% Sn alloy reinforced with low content of graphene nanoplatelets (GNPs)," *journal of Industrial and Engineering Chemistry,* vol. 20, pp. 4250-4255, 2014.

[292] P. Svoboda, C. Zeng, H. Wang, L. J. Lee, and D. L. Tomasko, "Morphology and mechanical properties of polypropylene/organoclay nanocomposites," *Journal of Applied Polymer Science,* vol. 85, pp. 1562-1570, 2002.

[293] S. K. Singh, A. Kumar, and A. Jain, "Improving tensile and flexural properties of SiO 2-epoxy polymer nanocomposite," *Materials Today: Proceedings,* vol. 5, pp. 6339-6344, 2018.

[294] T. Hsieh, A. Kinloch, K. Masania, A. Taylor, and S. Sprenger, "The mechanisms and mechanics of the toughening of epoxy polymers modified with silica nanoparticles," *Polymer,* vol. 51, pp. 6284-6294, 2010.

[295] B. Blackman, A. Kinloch, J. S. Lee, A. Taylor, R. Agarwal, G. Schueneman*, et al.*, "The fracture and fatigue behaviour of nano-modified epoxy polymers," *Journal of Materials Science,* vol. 42, pp. 7049-7051, 2007.

[296] N. R. Kumar and E. Dwarakadasa, "Effect of matrix strength on the mechanical properties of Al–Zn–Mg/SiCP composites," *Composites Part A: Applied Science and Manufacturing,* vol. 31, pp. 1139-1145, 2000.

[297] C. Lee, J. Huang, and P. Hsieh, "Mg based nano-composites fabricated by friction stir processing," *Scripta Materialia,* vol. 54, pp. 1415-1420, 2006.

Figure Captions List

Figure 1 Micro-features as applications of micromachining of nanocomposites. (a - b) SEM images of MTA/MWCNT micro-capacitors and micro-resistors made by precise 3D printing (Reprinted from [12] Copyright 2016, with permission from Society of Photo-Optical Instrumentation Engineers (SPIE)); (c) SEM image of a stainless steel/Al2O3 piston and a linkage rod made by soft molding (Reprinted from [22] Copyright 2009, with permission from Acta Materialia); (d) SEM image of a stainless steel/titania micro-gear made by soft molding (Reprinted from [23] Copyright 2009, with permission from Elsevier); (e) Optical image of a Epoxy/SiO2 wheel and (f) SEM image of a epoxy/SiO2 micro-gearwheel made by UV-LIGA methods (Reprinted from [229] Copyright 2009 , with permission Elsevier)

Figure 2 Normalized tensile modulus of epoxy-based composites as a function of micro-filler size (Adapted from [35-37], [230])

Figure 3 Normalized tensile modulus of polymer-based nanocomposites as a function of nano-filler size (Adapted from [231, 232])

Figure 4 Graphical representation of the effect of CNT aspect ratio while interacting with polymer chains (Reprinted from [46] Copyright 2015, with permission from Elsevier)

Figure 5 Theoretical models representing the micromechanical strengthening mechanism of polymer/CNT nanocomposites via the analysis of interfacial stress transfer with the consideration of various factors: (a)

Effects of polymer matrix density, chemical cross-links and CNT defect (Reprinted from [47] Copyright 2006, with permission from Elsevier); (b) Effects of SWCNT waviness (Adapted with permission from [48] Copyright © 2011 Elsevier); (c) Effects of tube length and diameter (Reprinted from [49] Copyright 2004, with permission from Woodhead Publishing); (d) Effects of nanotube aspect ratio and fiber volume fraction (Reprinted from [54] Copyright 2006, with permission from Elsevier)

Figure 6 (a) Effect of SWCNT's diameter, thickness and length on the stress transfer efficiency (δ); (b) Effect of Young's modulus on the stress transfer efficiency (δ) (Assumed that CF had the same hollow structure with d= 3nm and t= 0.142 nm as SWCNT) (Fiber volume fraction Vf ~ 0.17 %)(Reproduced from [49]); (c) Effect of nanotube diameter on stress transfer efficiency (Vf = 0.1%); (d) Effect of nanotube volume fraction on stress transfer efficiency (d = 0.7086 nm) (Reproduced from [54])

Figure 7 (a) Schematic of the microstructure of CNT-reinforced MMCs with DPZs. (b) The entire composite is decomposed into CNT and effective matrix phase, and the effective matrix is comprised of DPZs and pure metal matrix (Reprinted from [63] Copyright 2014, with permission from Elsevier)

Figure 8 Mechanical properties of polymers reinforced CNTs with corresponding dispersion techniques (Adapted from [94, 96, 100, 233-236])

Figure 9	Effects of dispersion method on mechanical properties of CNT reinforced PMNCs (Reproduced from [98])
Figure 10	Effect of CNT structure on mechanical properties of polymer nanocomposites at a filler content of 0.3 wt.% (Adapted from [117])
Figure 11	Effect of CNT alignment on mechanical properties of epoxy-based nanocomposites (Adapted from [237, 238])
Figure 12	Effect of CNT functionalization on tensile modulus of CNT reinforced epoxy matrix nanocomposites (Adapted from [80, 108, 117])
Figure 13	Fracture strain improvement of CNT based polymer nanocomposites as a function of filler content (Adapted from [94, 96, 109, 110, 239-241])
Figure 14	Schematic representing fracture toughening mechanism of CNT reinforced polymer nanocomposites (Reprinted from [113] Copyright 2017, with permission from Elsevier)
Figure 15	Normalized Young's moduli of TPU/graphene nanocomposites in different processing methods) (Adapted from [11])
Figure 16	Fracture strain improvement of graphene-based PMNCs as a function of filler content (Adapted from [164, 242-244])
Figure 17	Comparative fracture toughness improvement of epoxy-based nanocomposites using different nano-fillers [165] (Open access from The Royal Society of Chemistry)
Figure 18	Schematic representing fracture toughening mechanism of CNT reinforced PMNCs (Adapted from [152] Copyright 2015 The Authors – Open access from Elsevier)

Figure 19	The formation of carbide when fabricating metal/GO (2 wt.%) nanocomposites (Reprinted from [180] Copyright 2014, with permission from Acta Materialia)
Figure 20	The agglomerations of ceramic nano-particles in Al matrices: (a) Al/Al2O3 4 vol.% [217] and (b) Al/SiC 3 wt.% [216] (Open Access from Metals)

Table Caption List

Table 1	Nanocomposite manufacturing techniques
Table 2	Nano-filler geometries
Table 3	Fracture toughness of polymer reinforced CNT nanocomposites with the consideration of various factors
Table 4	Mechanical properties of CNT reinforced metal matrix nanocomposites
Table 5	Mechanical properties of graphene reinforced polymer matrix nanocomposites
Table 6	Mechanical properties of graphene reinforced metal matrix nanocomposites
Table 7	Mechanical properties of ceramic nano-fillers reinforced polymer matrix nanocomposites
Table 8	Mechanical properties of ceramic nano-particle reinforced metal matrix nanocomposites

Information Regarding Figures and Tables

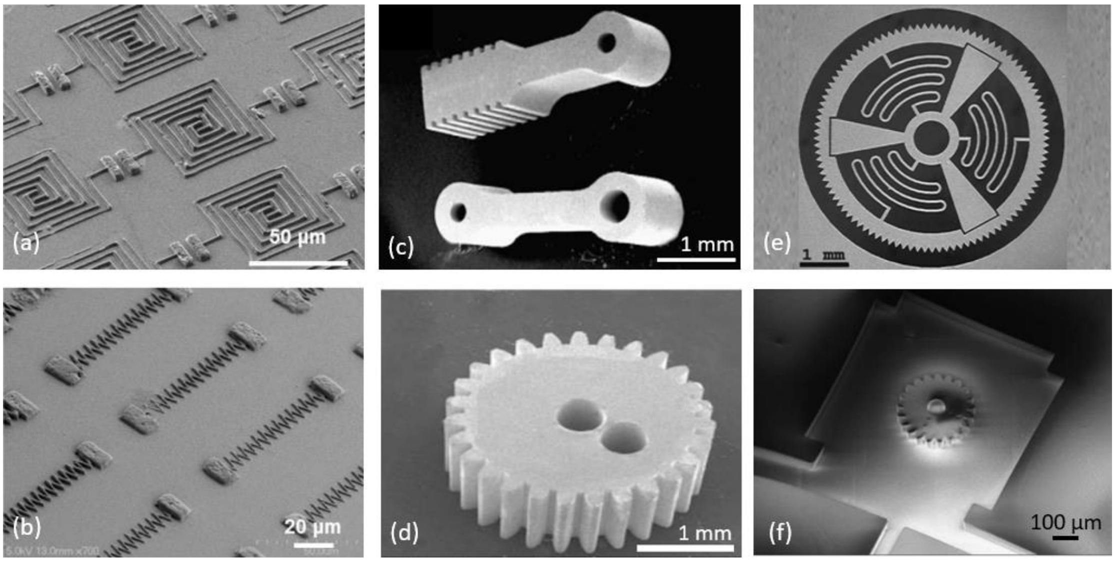

Figure 1: Micro-features as applications of micromachining of nanocomposites. (a - b) SEM images of MTA/MWCNT micro-capacitors and micro-resistors made by precise 3D printing (Reprinted from [12] Copyright 2016, with permission from Society of Photo-Optical Instrumentation Engineers (SPIE)); (c) SEM image of a stainless steel/Al2O3 piston and a linkage rod made by soft molding (Reprinted from [22] Copyright 2009, with permission from Acta Materialia); (d) SEM image of a stainless steel/titania micro-gear made by soft molding (Reprinted from [23] Copyright 2009, with permission from Elsevier); (e) Optical image of a Epoxy/SiO2 wheel and (f) SEM image of a epoxy/SiO2 micro-gearwheel made by UV-LIGA methods (Reprinted from [229] Copyright 2009 , with permission Elsevier)

MTA: thiol-acrylate; MWCNT: multi-walled carbon nanotube; SWCNT: single-walled carbon nanotube; PP: polypropylene

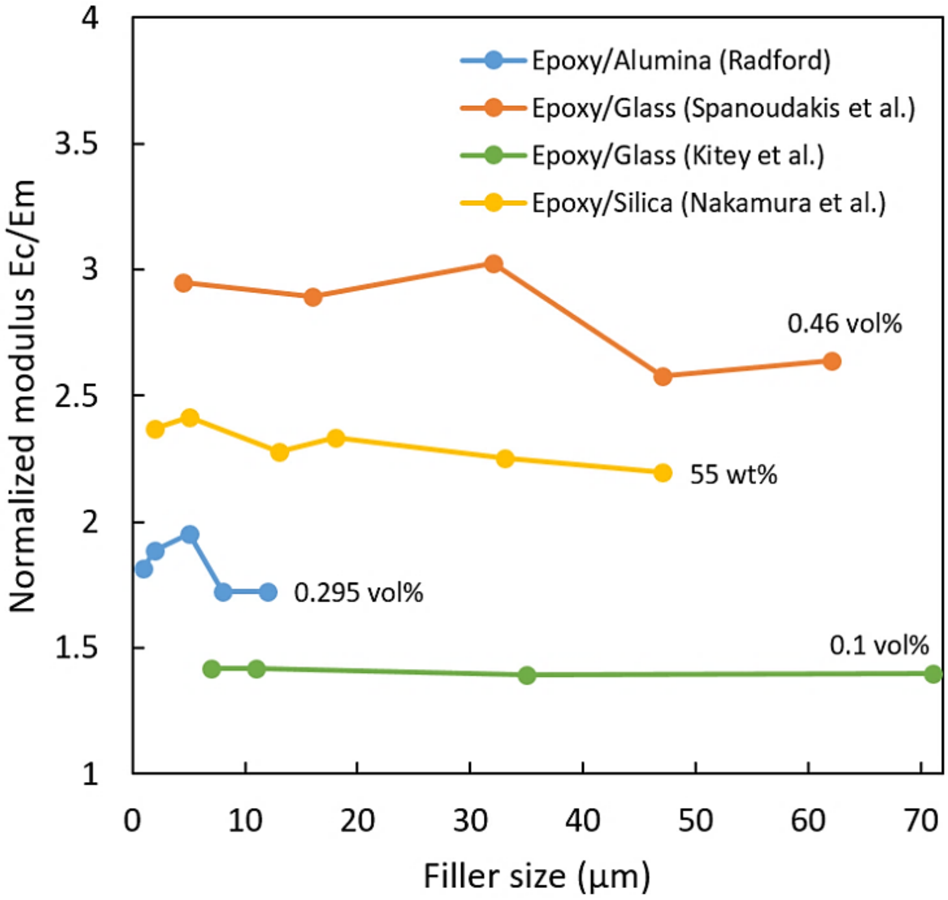

Figure 2: Normalized tensile modulus of epoxy-based composites as a function of micro-filler size (Adapted from [35-37], [230])

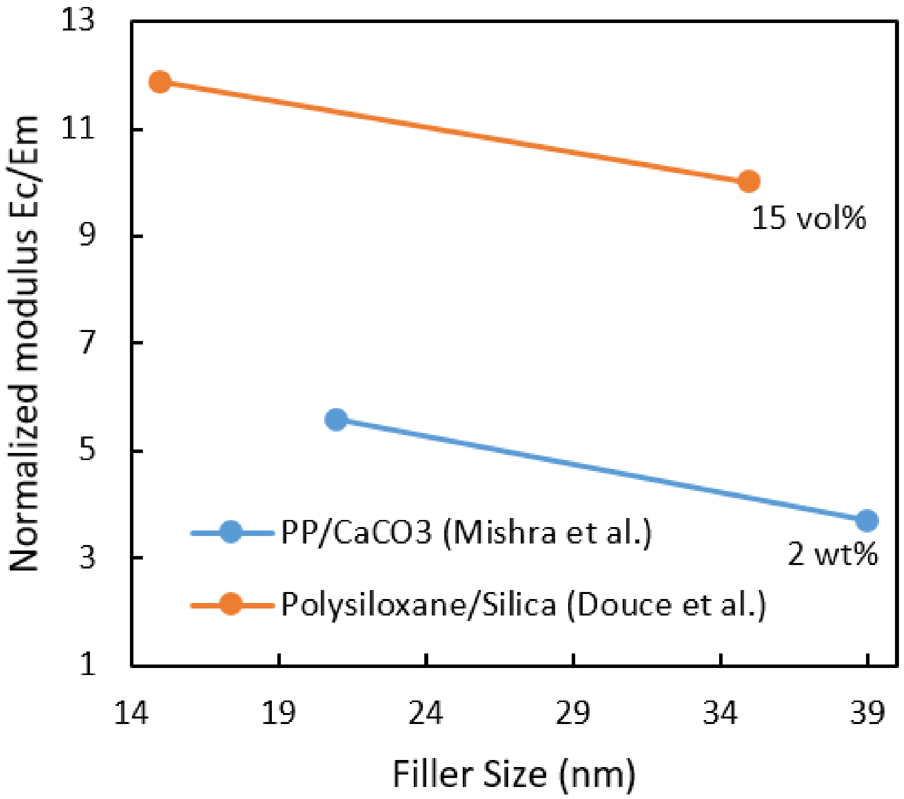

Figure 3: Normalized tensile modulus of polymer-based nanocomposites as a function of nano-filler size (Adapted from [231, 232])

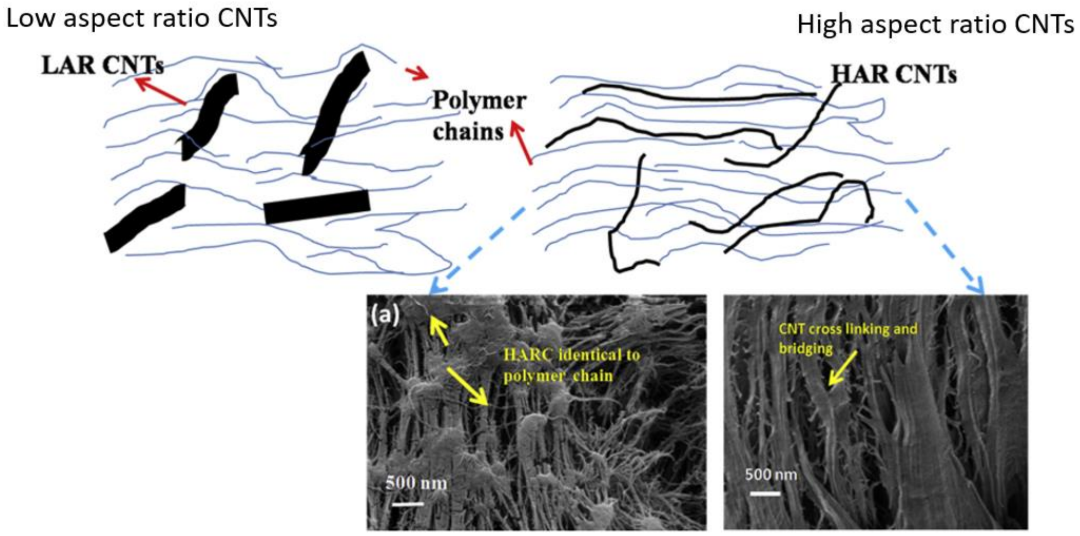

Figure 4: Graphical representation of the effect of CNT aspect ratio while interacting with polymer chains (Reprinted from [46] Copyright 2015, with permission from Elsevier)

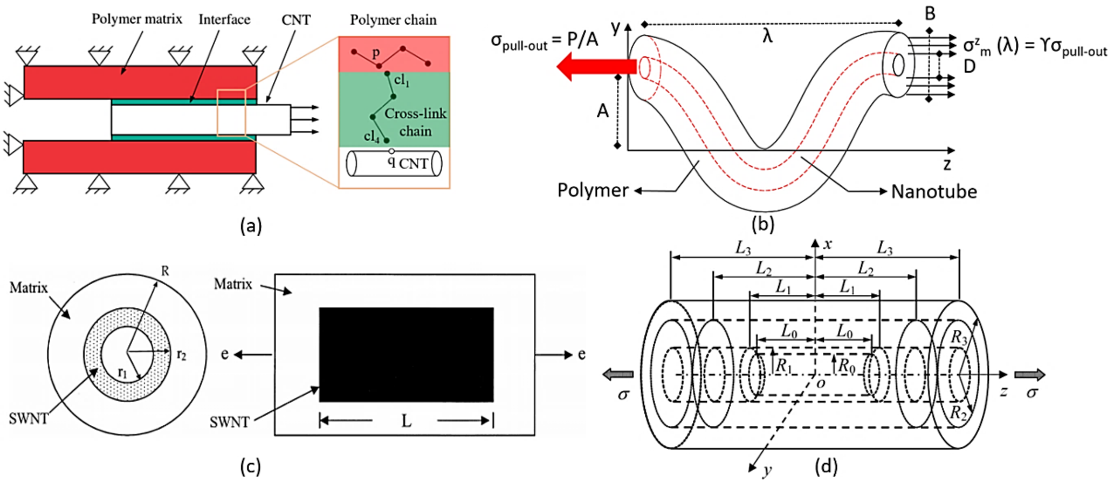

Figure 5: Theoretical models representing the micromechanical strengthening mechanism of polymer/CNT nanocomposites via the analysis of interfacial stress transfer with the consideration of various factors: (a) Effects of polymer matrix density, chemical cross-links and CNT defect (Reprinted from [47] Copyright 2006, with permission from Elsevier); (b) Effects of SWCNT waviness (Adapted with permission from [48] Copyright © 2011 Elsevier); (c) Effects of tube length and diameter (Reprinted from [49] Copyright 2004, with permission from Woodhead Publishing); (d) Effects of nanotube aspect ratio and fiber volume fraction (Reprinted from [54] Copyright 2006, with permission from Elsevier)

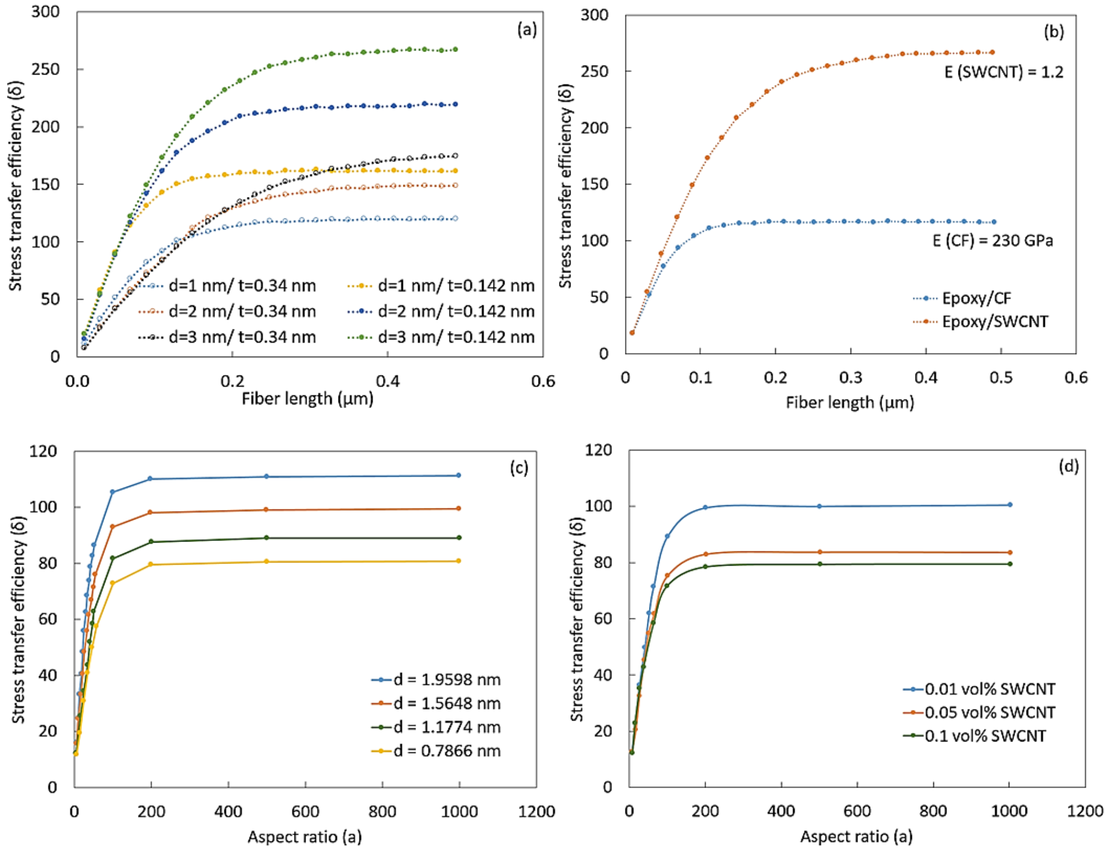

Figure 6: (a) Effect of SWCNT's diameter, thickness and length on the stress transfer efficiency (δ); (b) Effect of Young's modulus on the stress transfer efficiency (δ) (Assumed that CF had the same hollow structure with d= 3nm and t= 0.142 nm as SWCNT) (Fiber volume fraction V_f ~ 0.17 %)(Reproduced from [49]); (c) Effect of nanotube diameter on stress transfer efficiency (V_f = 0.1%); (d) Effect of nanotube volume fraction on stress transfer efficiency (d = 0.7086 nm) (Reproduced from [54])

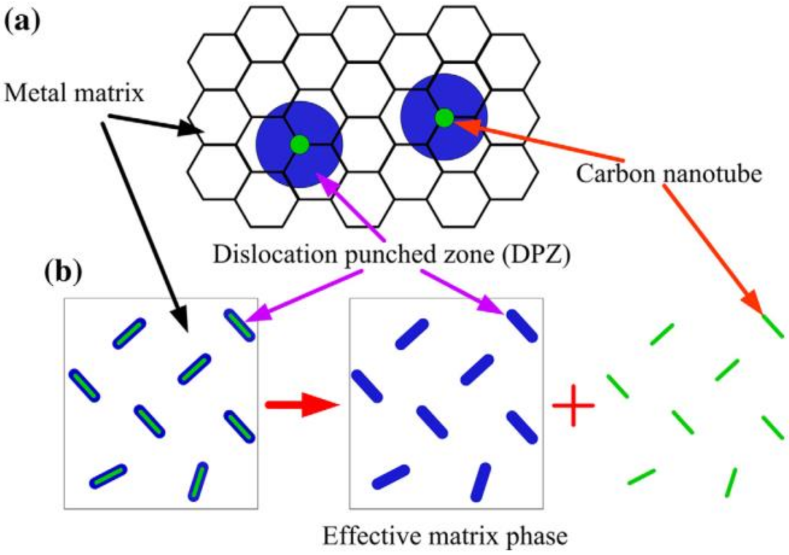

Figure 7: (a) Schematic of the microstructure of CNT-reinforced MMCs with DPZs. (b) The entire composite is decomposed into CNT and effective matrix phase, and the effective matrix is comprised of DPZs and pure metal matrix (Reprinted from [63] Copyright 2014, with permission from Elsevier)

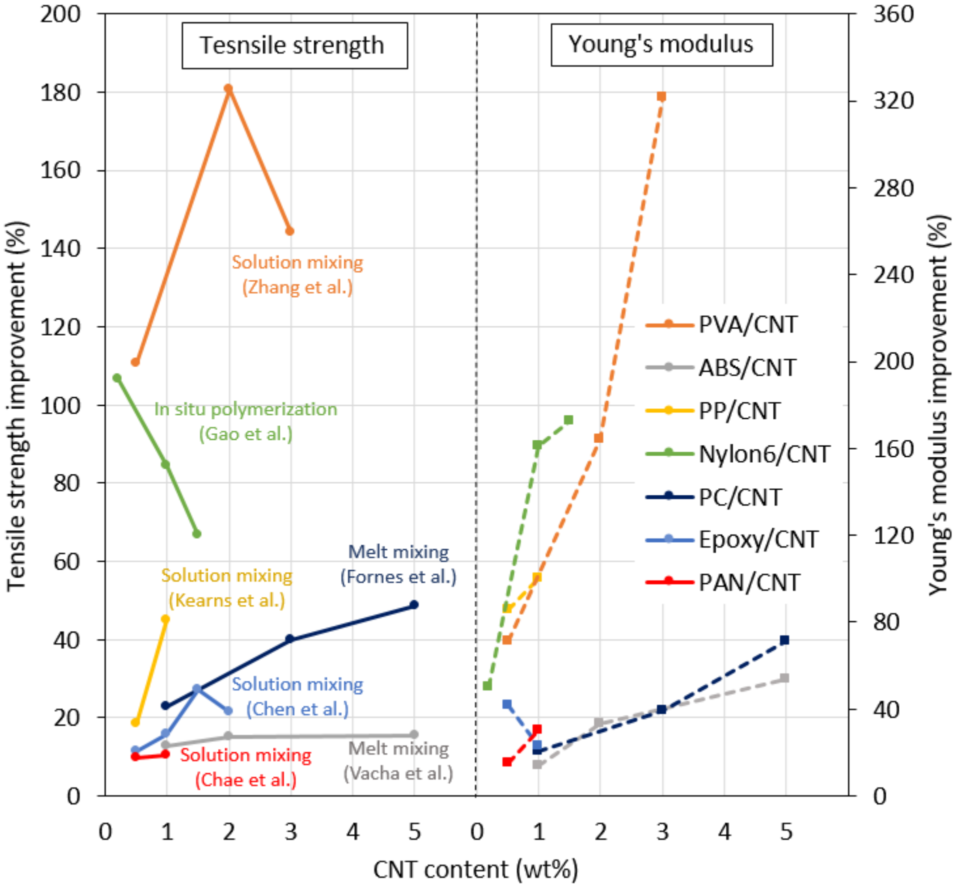

(ABS: Acrylonitrile butadiene styrene; PAN: Poly-acrylonitrile; HDPE: High-density Polyethylene)

Figure 8: Mechanical properties of polymers reinforced CNTs with corresponding dispersion techniques (Adapted from [94, 96, 100, 233-236])

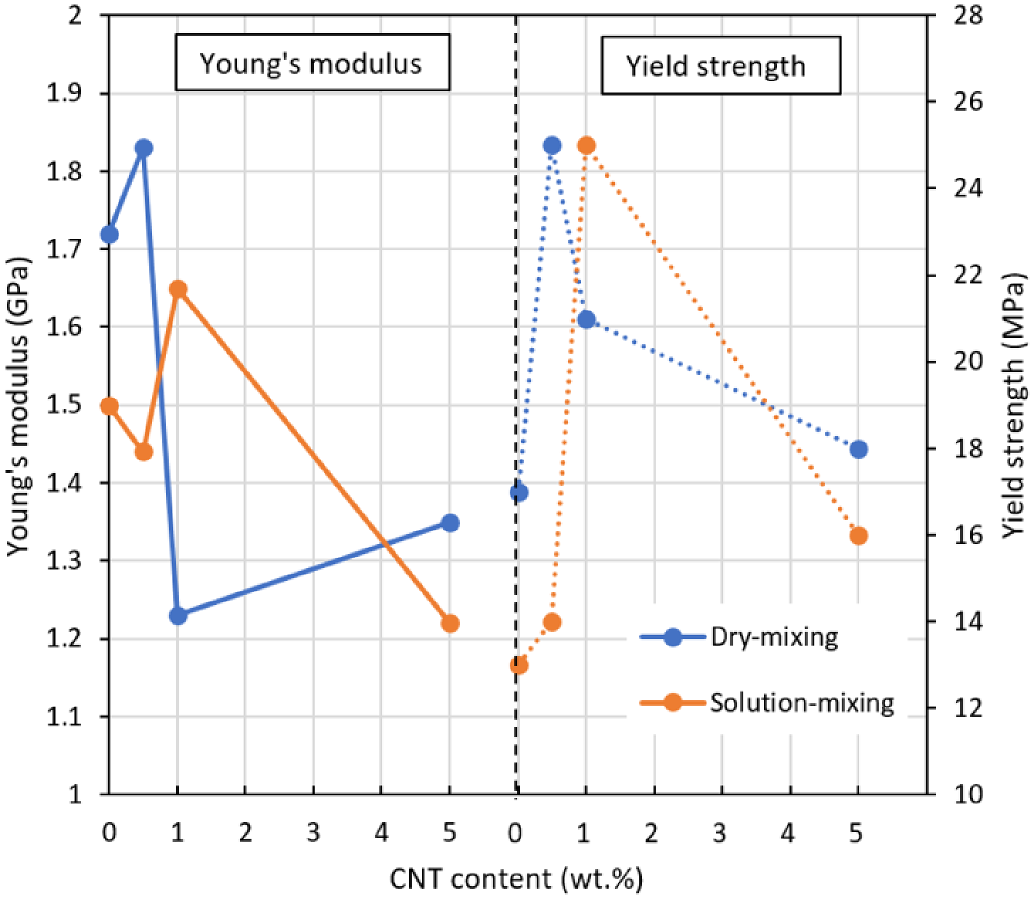

Figure 9: Effects of dispersion method on mechanical properties of CNT reinforced PMNCs (Reproduced from [98])

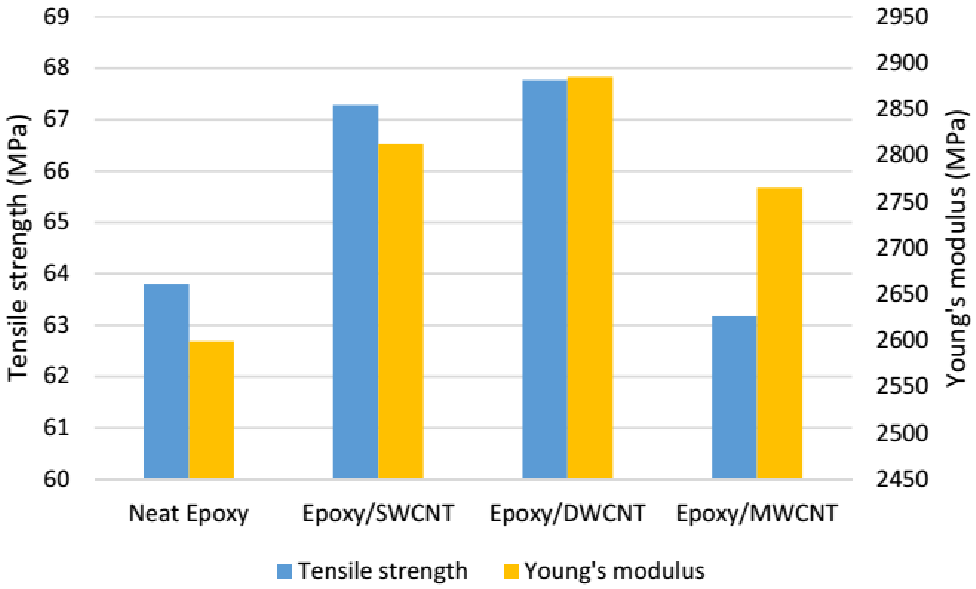

Figure 10: Effect of CNT structure on mechanical properties of polymer nanocomposites at a filler content of 0.3 wt.% (Adapted from [117])

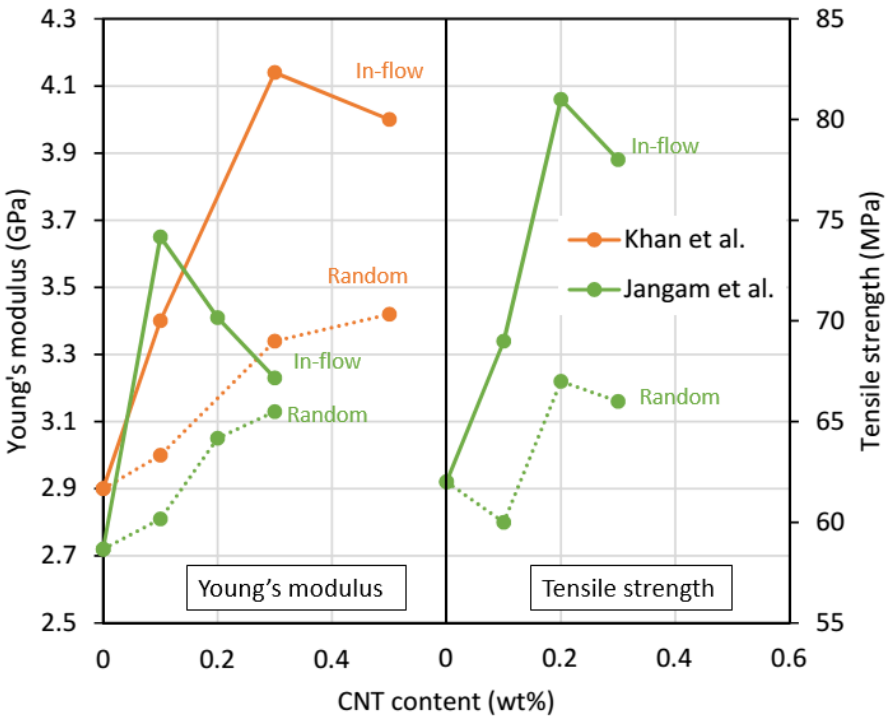

Figure 11: Effect of CNT alignment on mechanical properties of epoxy-based nanocomposites (Adapted from [237, 238])

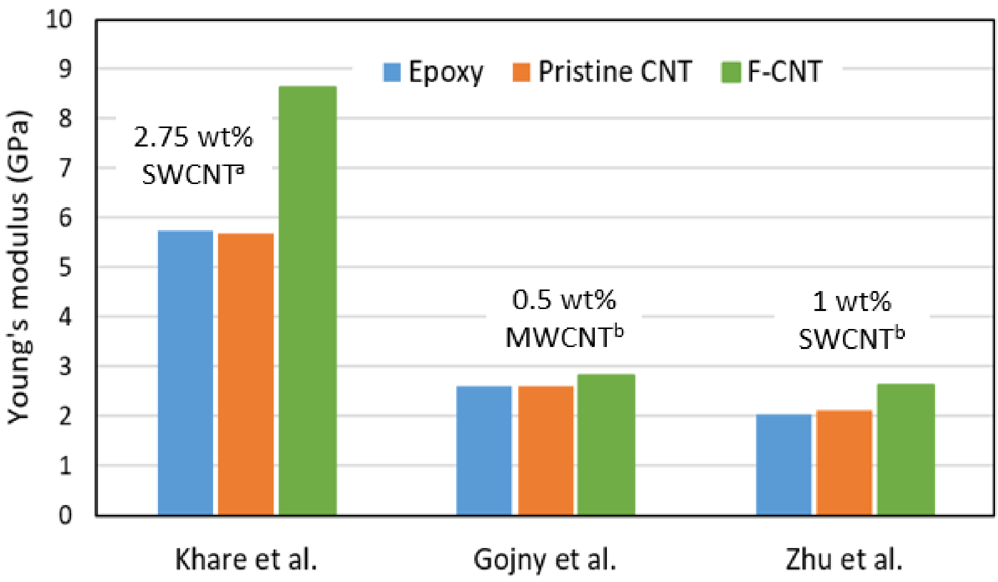

[a] Simulation result ; [b] Experimental result

Figure 12: Effect of CNT functionalization on tensile modulus of CNT reinforced epoxy matrix nanocomposites (Adapted from [80, 108, 117])

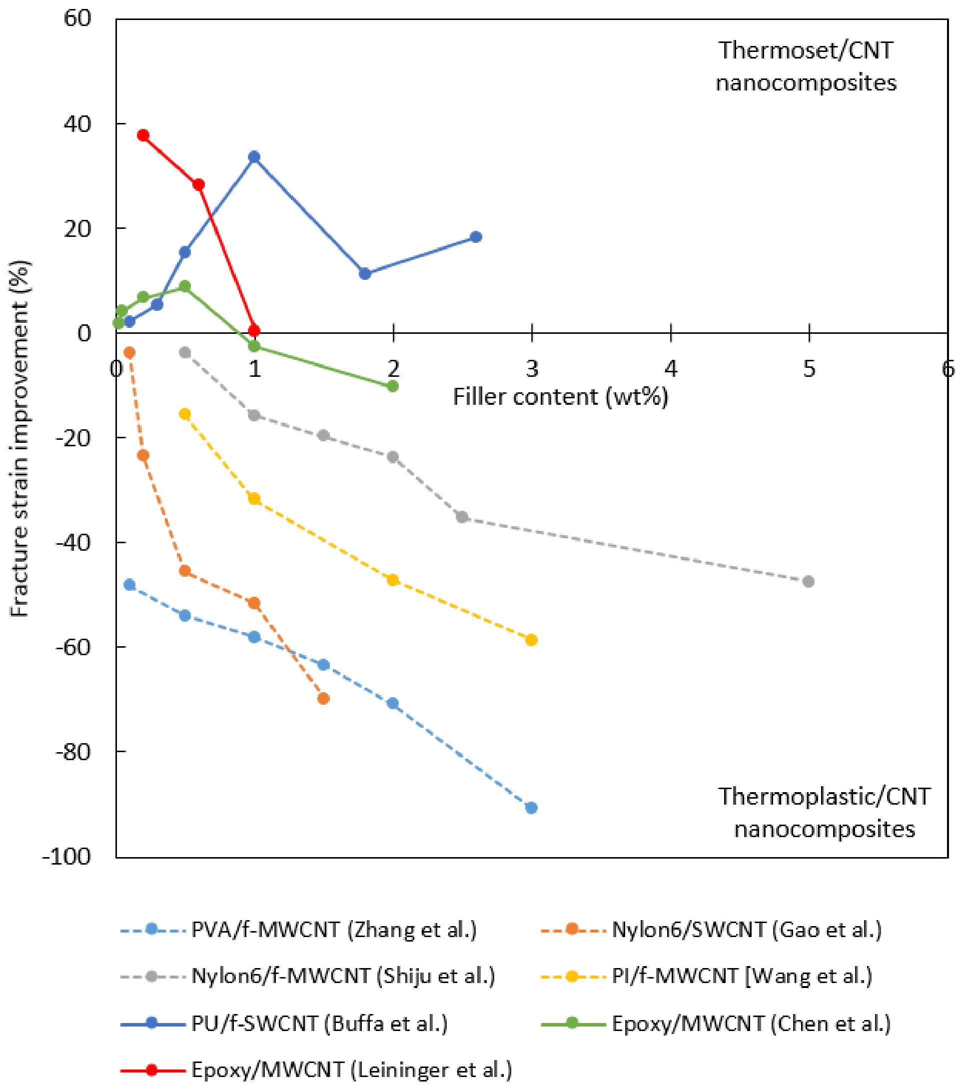

Figure 13: Fracture strain improvement of CNT based polymer nanocomposites as a function of filler content (Adapted from [94, 96, 109, 110, 239-241])

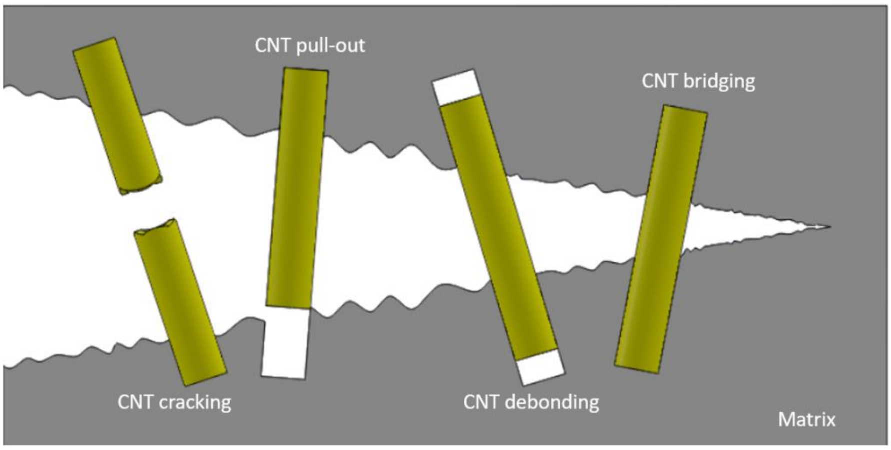

Figure 14: Schematic representing fracture toughening mechanism of CNT reinforced polymer nanocomposites (Reprinted from [113] Copyright 2017, with permission from Elsevier)

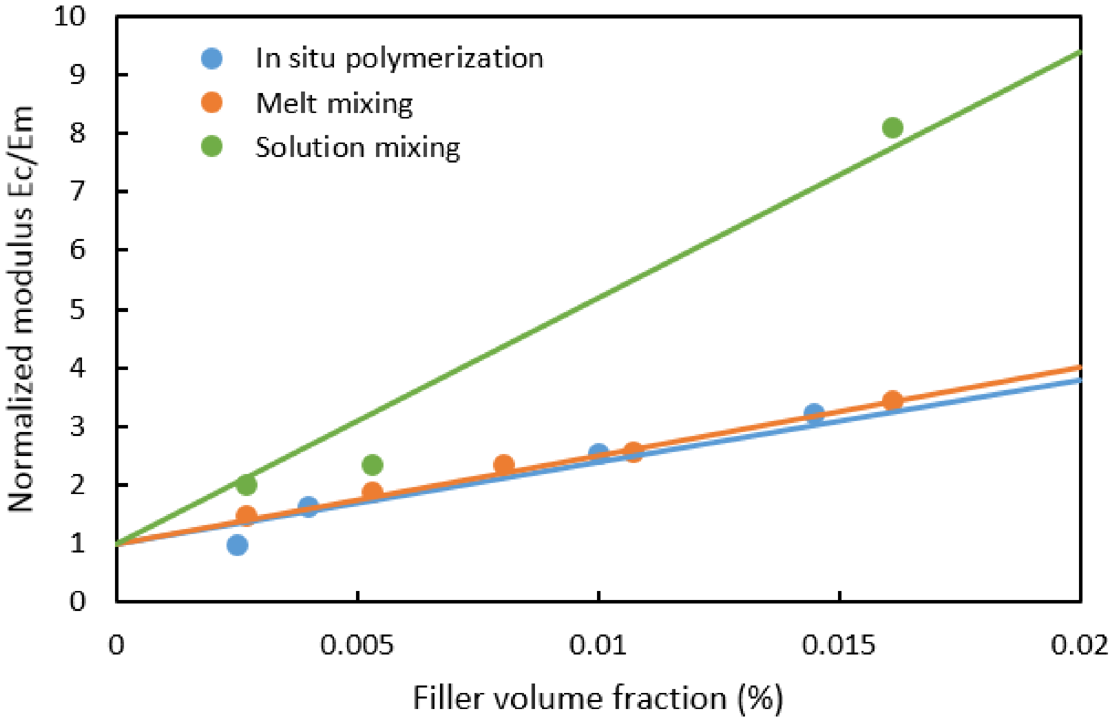

Figure 15: Normalized Young's moduli of TPU/graphene nanocomposites in different processing methods) (Adapted from [11])

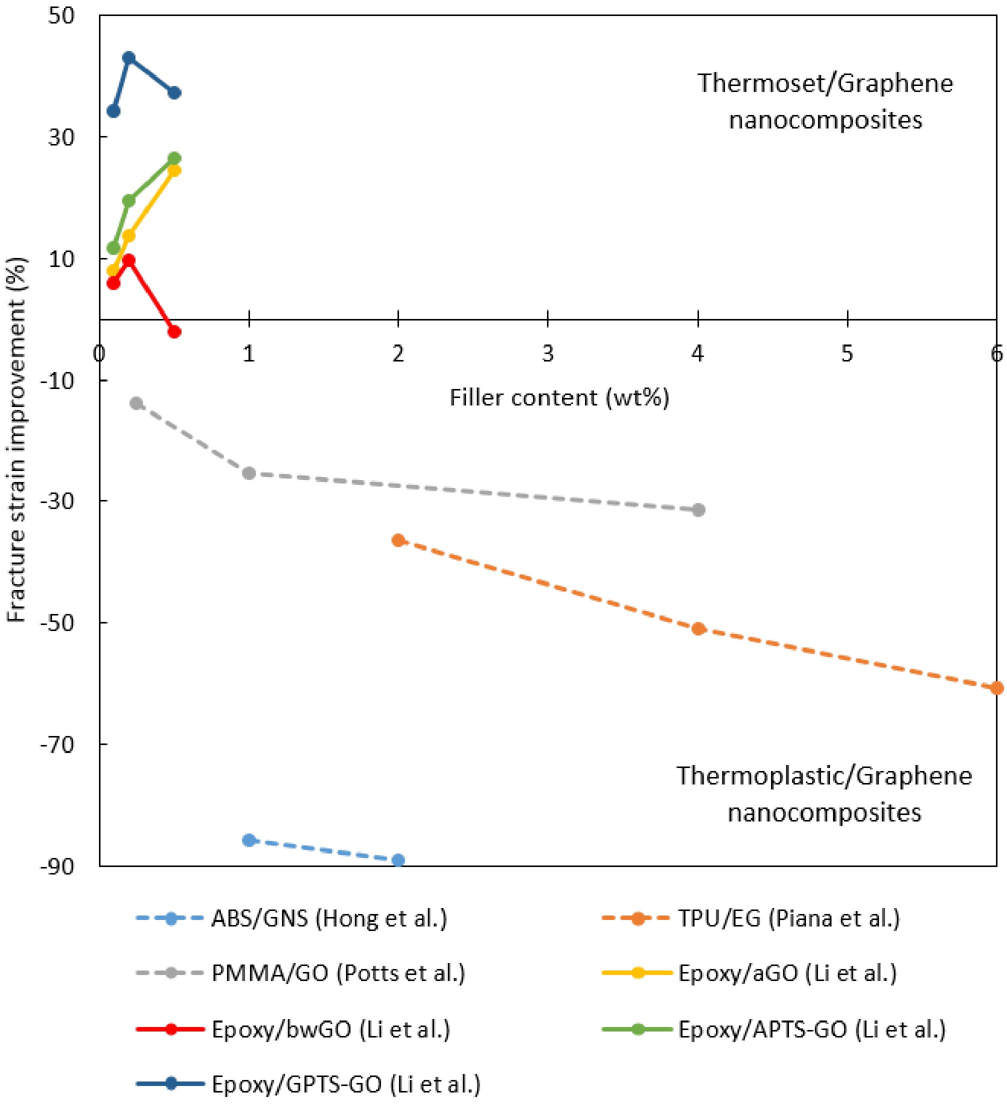

Figure 16: Fracture strain improvement of graphene-based PMNCs as a function of filler content (Adapted from [164, 242-244])

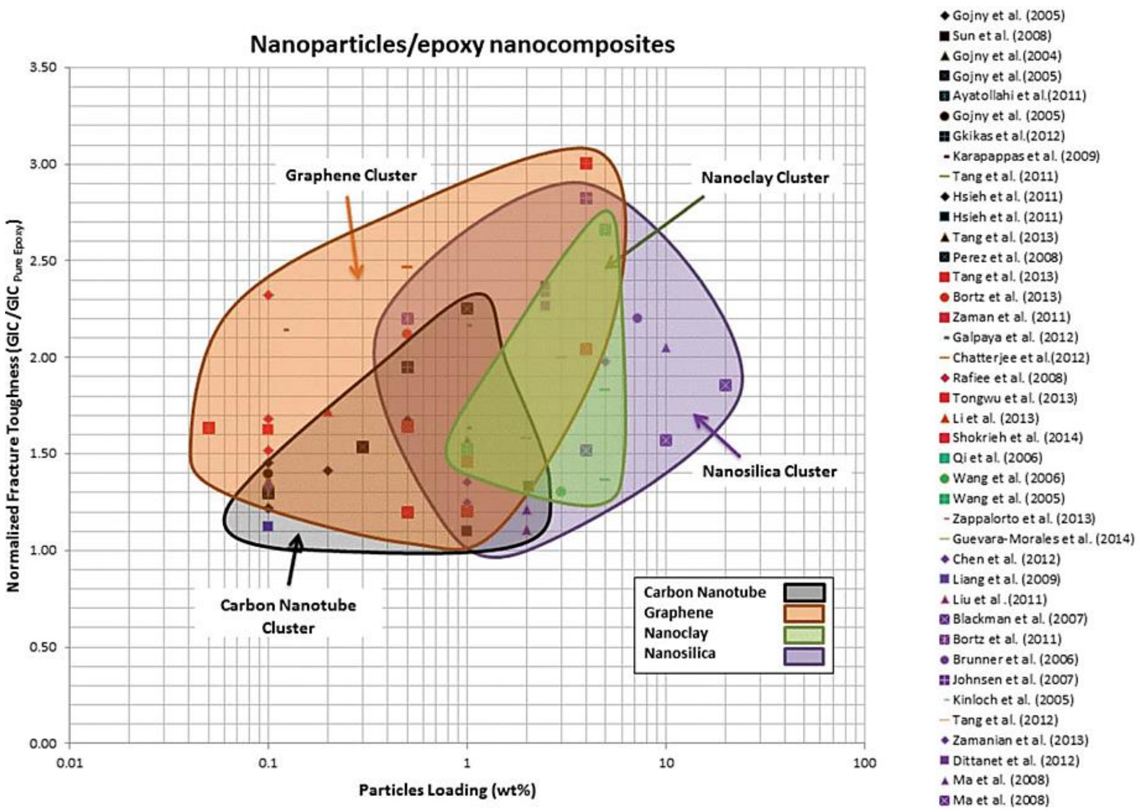

Figure 17: Comparative fracture toughness improvement of epoxy-based nanocomposites using different nano-fillers [165] (Open access from The Royal Society of Chemistry)

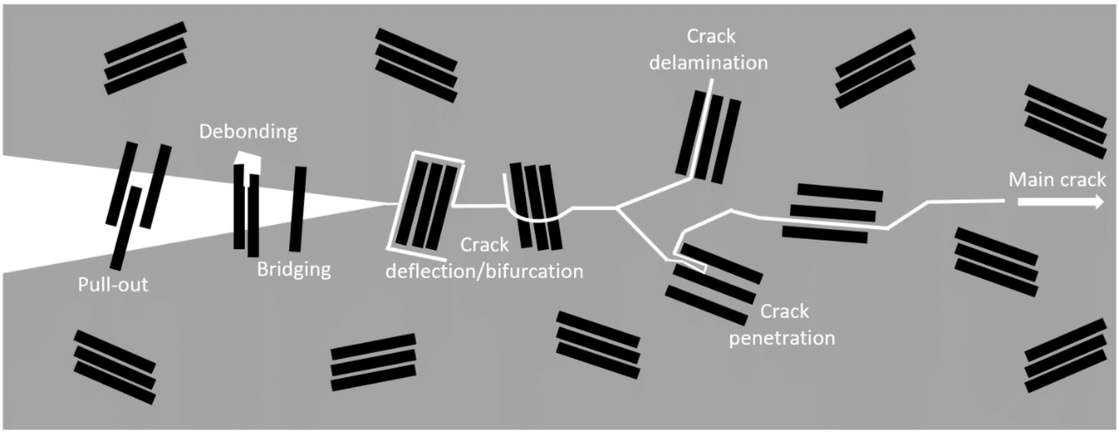

Figure 18: Schematic representing fracture toughening mechanism of CNT reinforced PMNCs (Adapted from [152] Copyright 2015 The Authors – Open access from Elsevier)

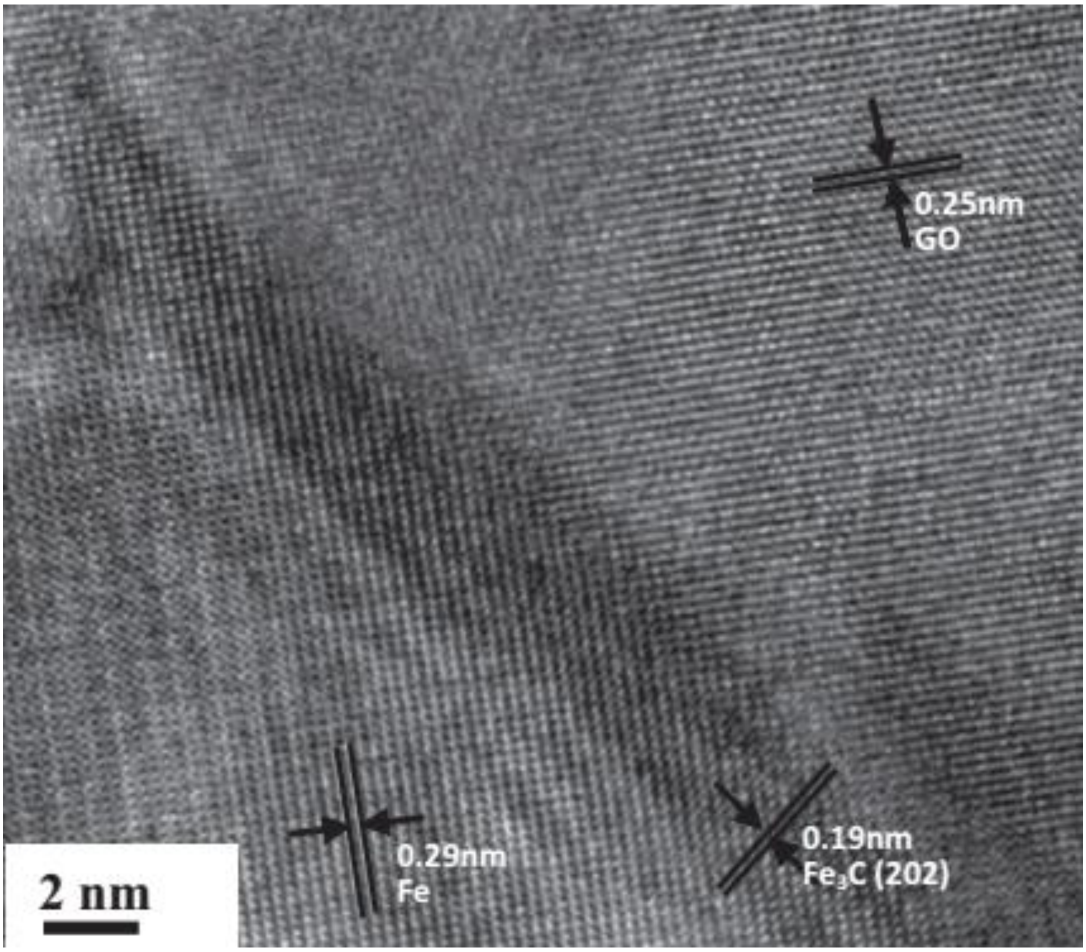

Figure 19: The formation of carbide when fabricating metal/GO (2 wt.%) nanocomposites (Reprinted from [180] Copyright 2014, with permission from Acta Materialia)

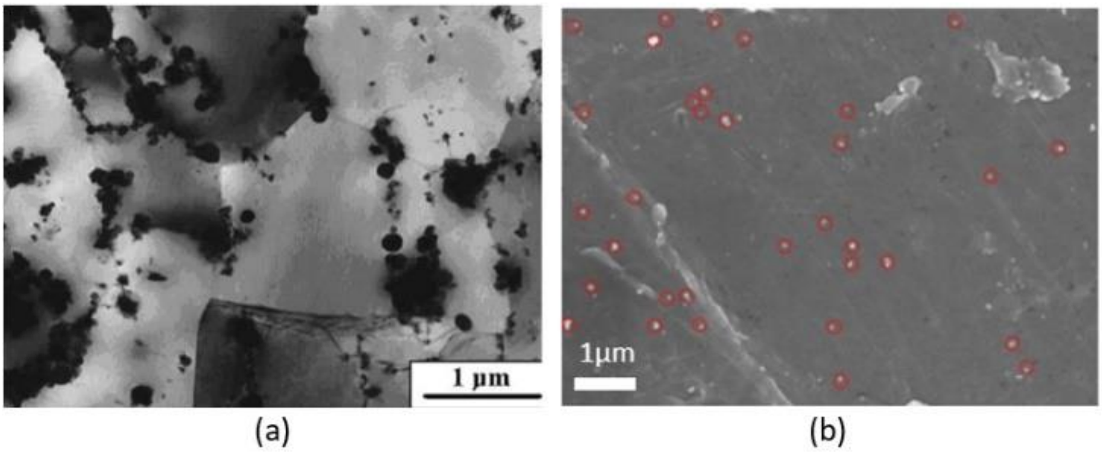

Figure 20: The agglomerations of ceramic nano-particles in Al matrices: (a) Al/Al_2O_3 4 vol.% [217] and (b) Al/SiC 3 wt.% [216] (Open Access from Metals)

Table 1: Nanocomposite manufacturing techniques

Nanocomposites	Manufacturing method	Ref.
Polymer matrix nanocomposites (PMNCs)	Melt mixing	[245]
	Solution mixing	[246]
	In situ polymerisation	[247]
	In situ formation	[248]
	Sol-Gel	[249]
Metal matrix nanocomposites (MMNCs)	Spray pyrolysis	[250]
	Infiltration	[251]
	Rapid solidification	[252]
	High energy ball milling and powder metallurgy (consolidation)	[253]
	Chemical vapour deposition	[254]
	Physical vapour deposition	[255]
	Colloidal suspension	[256]
	Sol-Gel and hot pressing	[257]
Ceramic matrix nanocomposites (CMNCs)	Powder processing (Compression, rolling, and extrusion)	[258]
	Polymer precursor	[259]
	Sol-Gel and consolidation	[260]

Table 2: Nano-filler geometries

1D-Planar shape	2D-Tubular shape	3D- Spherical shape
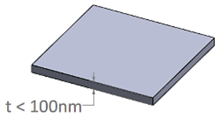	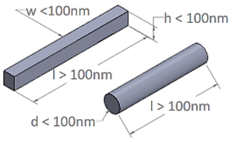	
at least one dimension ≤ 100 nm	at least two dimensions ≤ 100nm	all three dimensions ≤ 100nm
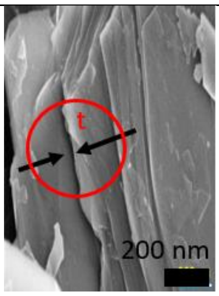	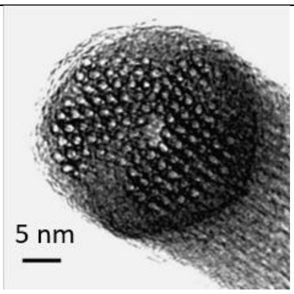	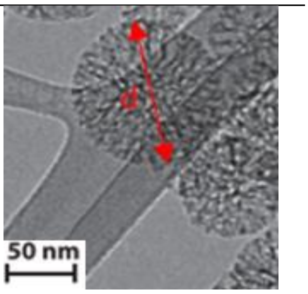
Graphene [261]	SWCNT (Reprinted with permissons from [262] Crown copyright © 2004)	Silica (Reprinted with permissons from [263] Copyright © 2016 Elsevier)

Table 3: Fracture toughness of polymer reinforced CNT nanocomposites with the consideration of various factors

Matrix	Factors	Variables	Filler content (wt.%)	Fracture toughness Improvement (%)	Ref.
Epoxy	- CNT structure -Functionalization - Filler content	SWCNT	0.05	10.8	[117]
			0.1	23.0	
			0.3	12.3	
		DWCNT	0.1	16.9	
			0.3	30.8	
			0.5	30.7	
		DWCNT-NH_2	0.1	18.5	
			0.3	41.5	
			0.5	43.0	
		MWCNT	0.1	21.5	
			0.3	23.0	
		MWCNT	0.1	24.6	
			0.3	30.8	
			0.5	29.2	
Epoxy	- CNT diameter	Type A (20-30 nm)	0.5	31.8	[264]
		Type B (30-40 nm)		26.4	
		Type C (40-50 nm)		24.2	
		Type D (50-60 nm)		21.2	
Epoxy	- CNT length	2091 nm	0.1	46.6	[265]
		1689 nm		43.3	
		1332 nm		8.7	
		992 nm		2.0	
		503 nm		-14.7	
Epoxy	- CNT alignment - Filler content	Random orientation	0.05	6.2	[237]
			0.1	11.6	
			0.3	16.9	
			0.5	13.8	
		Aligned orientation	0.05	23.3	
			0.1	36.1	
			0.3	53.0	
			0.5	31.1	
Epoxy		Three-Roll Milling	0.1	58.3	[266]
			0.5	64.5	

	-Processing technique	(TRM)	1	68.5	
			1.5	60.0	
			2	57.7	
		HPH (High Pressure Homogenization)	0.1	48.3	
			0.5	56.4	
			1	64.2	
			1.5	56.0	
			2	42.0	
		HPH + TRM	0.1	82.6	
			0.5	72.5	
			1	78.5	
			1.5	78.0	
			2	74.0	

Table 4: Mechanical properties of CNT reinforced metal matrix nanocomposites

Material	Tensile strength (MPa)	Young's modulus (GPa)	Hardness (GPa)	Elongation (%)	Reasons	Fabricating methods
Al/MWCNT 1wt.% [139]	521.7 (35.7%)	102.2 (41.3%)	0.136 (30.8%)	17.9 (-5%)	Good interfacial bonding, homogenous distribution, high elastic behavior of CNT, integrality of Al	Powder metallurgy cold isostatic press, hot extrusion
Al/MWCNT 0.5wt.% [138]	130 (9.2%)	60 (20%)	--	18.7 (-25.8%)	Good distribution of CNT due to rolling process	Mechanical mixing, hot rolling
Al/(Si) MWCNT 10wt.% [143]	83.1 (4%)	120.4 (78%)	--	8.8E-4 (-54%)	Strengthening by retained CNT and nano-crystalline structure	Thermal spray, plasma spraying (SPS)
Al/(Si) CNT 10wt.% [267]	--	125 (39%)	2.1 (141%)	--	Good distribution of CNTs due to Si-coating and dispersing method	Spark plasma sintering (SPS)
Al/(Ni) CNT 5wt.% [132]	213 (52%)	--	3200 (113.3%)	--	Homogenous dispersion, CNT structure retention, strong interfacial strength due to molecular mixing in in-situ CVD synthesis as compared to ball milling	Ball milling
	398 (184%)	--	6.5 (333%)	--		In situ CVD synthesis
Cu/MWCNT 20 vol.% [137]	--	106.5 (108%)	1.304 (72%)	--	Homogenous distribution and reduction of MWCNT agglomerations	SPS and electroless deposition
Cu/MWCNT 10 vol.% [136]	196 (45%)	135 (95%)	1.75 (207%)	--	Homogenous distribution of CNT	SPS, cold rolling
Cu/(Ni) CNT 12 vol.% [268]	--	--	21.5[a] (111%)	--	Highest mechanical reinforcement at 12 vol.% of CNT	Mechanical mixing and hot pressing
Cu/(Ni) MWCNT 0.75wt.% [140]	279 (76%)	--	1.383 (54%)	--	CNTs resist plastic deformation, thermal expansion mismatch, homogenous distribution, good interfacial bonding, high hardness of Ni	Ball milling and hot pressing
Cu/MWCNT 0.5 vol.% [269]	307.4 (81.6%)	--	106 (14.7%)	38.44 (55%)	Well dispersed of MWCNTs Stable interface blocks dislocation	Ball milling and hot pressing
Ni-P/MWCNT 0.21wt.% [270]	--	665.9 (303%)	28.9 (331%)	--	Strengthening effects due to MWCNT presence	Electroless deposition
Ni/MWCNT 0.1wt.% [271]	1140.7 (14.2%)	--	4.824 (74.5%)	7.69 (-29.7%)	High quality dispersion and integrity of MWCNT due to surfactant treatment	SPS

Mg-Zn/CNT 1 vol.% [142]	321 (13.6%)	52 (42.5%)	--	17 (-54.5%)	Homogenous, single distribution of CNTs, no reaction at interface, grain refinement	Melting and solidification
Mg/(Si)MWCNT 5 vol.% [134]	296 (44.4%)	--	1.569 (100%)	1.3 (-74%)	High wettability of MWCNTs due to Si-coating leads to good distribution, bonding strength	Ball mill and hot pressing
Mg/CNT 1.3wt.% [272]	210 (9%)	--	46[b] (2.2%)	--	The coefficient mismatch of thermal expansion and elastic modulus of Mg-CNT	Melt deposition and hot extrusion
Mg/(Ni) MWCNT 0.3wt.% [133]	237 (38.6%)	--	0.54 (41%)	--	Improved adhesion of Mg-(Ni)MWCNT due to Ni coating leading to Mg_2Ni intermetallic formation, grain refinement	Powder metallurgy, microwave-assisted sintering
Mg alloy/MWCNT 2wt.% [273]	297 (6.1%)	--	0.8 (0.37%)	9.2 (-36%)	Strengthening mechanism, thermal mismatch of CNT-Mg alloy	Ball mill, hot compact

[a]: HRB; [b]: HR15T

Table 5: Mechanical properties of graphene reinforced polymer matrix nanocomposites

Material	Tensile Strength (MPa)	Young's modulus (GPa)	Reasons	Fabricating methods
EP/GNP 0.3 wt.% [274]	64.4 (12.6%)	2.16 (30%)	The high temperature in low viscosity system, low concentration of Gr leading to low agglomeration and uniform distribution of Graphene	Solution mixing
EP/APTS-GO 0.2 wt.% [244]	81.2 (16%)	3.3 (32%)	Uniformly distributed APTS-GO, strong interfacial stress	Solution mixing
EP/NH$_2$-GNP 4 wt.% [275]	66 (1.5%)	3.4 (17%)	GNP aggregation, poor GNP dispersion	Solution mixing
EP/EGS 3 wt.% [276]	41 (20%)	3.7 (25%)	High aspect ratio and uniformly distributed EGS, good interfacial adhesion of EP-EGS	Solution mixing
EP/RGO 0.2 wt.% [277]	52.6 (-0.8%)	3.1 (7%)	Weak interfacial bond of EP-RGO, RGO agglomeration, RGO curvature	Solution mixing
EP/GNP 0.1 wt.% [278]	78 (40%)	3.7 (31%)	The high specific surface area of GNPs, strong matrix-filler adhesion/interlocking due to wrinkled surface of GNPs	Solution mixing
EP/GNP 0.3 wt.% [279]	70.4 (23%)	1.28 (47%)	High effect of Sodium Dodecyl Sulphate (SDS) as solution on GNP dispersion, effect of surfactants	Solution mixing
ABS/CO(OH)$_2$/ GNS 4 wt.% [242]	43.2 (50%)	--	High modulus GNS, homogenous dispersion	Melt mixing
PMMA/GO 1 wt.% [243]	70.9 (22%)	4.39 (28%)	High aspect ratios and good dispersions of GO at low loading, wrinkled platelets	In situ polymerization
PC/FLG 1 wt.% [280]	60 (10%)	1.45 (26%)	Optimizing the aspect ratio of the graphene flakes	Solution mixing
HDPE/GNS 3 wt.% [281]	47 (77%)	2.033 (87%)	High specific area and flat-structure of GNS, the mechanical interlocking of HDPE-GNS, enlarging the interphase zone	Melt mixing
LDPE/RGO 5 wt.% [282]	--	10.1 (60.7%)	Homogeneous distribution of exfoliated carbon sheets in functionalized PE	Solution mixing/ melt compounding
TPU/EG 10 wt.% [164]	9 (-84%)	0.091 (237%)	Homogenous distribution, HS crystallization, EG hindering the amorphous phase, weak interfacial interaction of TPU-EG, EG agglomerations	Melt mixing
PVA/GNS 3 wt.% [162]	43.2 (122%)	1.186 (155%)	Homogenous distributed Gr and strong interfacial interaction of PVA-GNP. GNP restricting polymer chain movements	Solution mixing

APTS-GO: amino-functionalized – graphene oxide; EGS: Graphene stack; FLG: Few layer graphene sheets; EG: Expanded graphite; GO: Graphene oxide; RGO: Reduced graphene oxide; GNP: Graphene nano-platelet; GNS: Graphene nano-sheet; GNP: Graphene nano-platelet

Table 6: Mechanical properties of graphene reinforced metal matrix nanocomposites

Material	Tensile Strength (MPa)	Young's modulus (GPa)	Hardness (GPa)	Elongation (%)	Reasons	Fabricating methods
Al/RGO 0.3wt.% [172]	--	90.1 (18%)	1.59 (17%)	--	High quality of RGO, uniform dispersed of RGO, strong interfacial bonding of Al-RGO	Compacting and hot pressing
Al-Mg-Cu/Gr 0.3wt.% [283]	454 (25%)	72 (-1%)	--	11.8 (7%)	Evenly distributed of Gr, good interfacial bonding, Gr structure retention	Ball milling, hot isostatic pressing (HIP) and extruding
Al/GO 15 mg ml^{-1} [284]	192 (-7%)	--	--	28 (50%)	Dynamic recrystallization of matrix phase due to shear deformation, heat from FSP and grain refinement	Friction stir processing (FSP)
Al/GNS 1 wt.% [285]	248 (68.7%)	--	--	8.3 (-52%)	Homogenous distribution of GNFs, no metallurgical at interfaces of Al-GNF	Blending, cryo-milling, degassing and hot extrusion
Cu/FLG 3 wt.% [286]	--	--	0.46 (39%)	16 (-71%)	Disruption of Gr layers due to Cu deformation by rolling, Gr partly hinder grain growth	Rolling
Cu/RGO 2.5 vol.% [184]	335 (30%)	131 (30%)	--	--	Strong interfacial bonding of Cu-RGO	Compacting and SPS
Cu/GO 0.5 gL^{-1} [287]	--	137 (30%)	2.5 (96%)	--	Uniform distribution of Gr, grain size refinement	Pulse reverse electrodeposition
Cu/(Ni)GPL 0.8 vol.% [288]	245 (42%)	--	--	9 (-67.8%)	Good dispersion of GPL and strong interfacial bonding Cu-GPL (Ni), covalent interaction of Ni-GPL	Solution, sonication, SPS
Cu/(Ni)GNS 1 vol.% c	320 39.1%)	132 (61%)	--	--	Homogenous dispersion of GPL and strong interfacial interaction of Cu-GPL due to Ni coating	Solution, sonication, SPS
Cu/GNP 1.3 wt.% [289]	485 (107%)	104 (21%)	--	9 (-64%)	Homogenous dispersion of GNPs due to pre-coating of Cu on GNPs	Electroless plating, SPS tensile
Cu/RGO 0.3 wt.% [290]	308 (41%)	109 (12%)	--	--	Less structural damage on RGO, randomly oriented of RGO benefit the load transfer of nanocomposite	Hot pressing
Ni/GO 0.12 wt.% [174]	--	252.76 (51.6%)	6.85 (278.4%)	--	Compact interfacial bonding of Ni-GO, homogenous dispersion of GO	Electrodeposition
Ni/Gr 0.05 gL^{-1} [179]	--	240 (70%)	4.6 (20%)	--	High interaction of Ni-Gr, Gr preventing Ni dislocation	Electrochemical deposition
Mg/Ti/GNP 0.18 wt.% [188]	230 (8.5%)	--	--	14 (27%)	High specific area and adhesion of Gr	Semi powder metallurgy
Mg-Al-Sn/ GNP 0.18 wt.% [291]	269 (14%)	--	--	10.9 (-34.7%)	High specific surface area, superior nano-filler adhesion and two-dimensional structure of GNPs	Semi-powder metallurgy

Mg/GNP 0.3 wt.% [173]	246 (32.2%)	13.84 (131%)	55HV (34%)	16.9 (74.2%)	High specific surface area of GNPs, uniform dispersion	Compaction, sintering, extruding

Table 7: Mechanical properties of ceramic nano-fillers reinforced polymer matrix nanocomposites

Material	Tensile Strength (MPa)	Young's modulus (GPa)	Reasons	Fabricating methods
PP/MMT 15 wt.% [292]	38 (13%)	3.36 (100%)	Well-dispersed MMTs	Melt mixing, injection molding
PP/MMT 10 wt.% [199]	41.6 (38.7%)	--	The intercalation of MMT layers in the matrix due to the presence of MAPP compatibilization	Melt mixing, injection molding
PP/MMT 2 wt.% [203]	32 (18%)	0.9 (82%)	The persistence of silicate layers, modification of PP structure, partially immobilized polymer segments	Melt mixing
PA6/MMT 7.2 wt.% [204]	--	5.7 (107%)	High molecular weight and integrity of matrix	Melt mixing
SPU/30B 7 wt.% [205]	21 (-53.3%)	0.024 (220%)	Well-dispersed and delaminated of Cloisite 30B regardless processing methods, good interaction of PU-clay, preferable solution mixing due to PU and surfactant degradations from melt mixing, larger improvements of the stiffness of SPU due to higher fraction of soft segment	Solution mixing Melt mixing
HPU/30B 7 wt.% [205]	34 (-41.3%)	0.134 (168%)		
SPU/30B 7 wt.% [205]	7 (-66.7%)	0.0193 (168%)		
HPU/30B 7 wt.% [205]	15 (-66%)	0.119 (95%)		
EVA/ Cloisite Na 3 wt.% [201]	25.9 (-8.8%)	0.0135 (10.7%)	The dominant effect of exfoliation on tensile properties of nanocomposites, high interaction between EVA and Cloisite 30B	Melt mixing, compression molding
EVA/ Cloisite 20A 3 wt.% [201]	25.8 (-9.2%)	0.0249 (104.1%)		
EVA/ Cloisite 25A 3 wt.% [201]	26.2 (-7.7%)	0.022 (80.3%)		
EVA/ Cloisite 30B 3 wt.% [201]	30.7 (8.1%)	0.0228 (86.9%)		
EVA/ Nanofile 757 3 wt.% [201]	27.6 (-2.8%)	0.0116 (-4.9%)		
EVA/ Nanofile 15 3 wt.% [201]	26.7 (-6%)	0.024 (96.7%)		
EVA/ Somasif ME100 3 wt.% [201]	24.5 (-13.7%)	0.0124 (1.6%)		
EVA/ Somasif MAE 3 wt.% [201]	25.1 (-11.6%)	0.021 (72.1%)		
EP/SMC 2 wt.% [200]	57 (25%)	3.3 (10%)	Homogenous distribution and high exfoliation of SMCs	Solution mixing
EP/SiO_2 3.72 vol.% [206]	--	3.96 (12%)	Less agglomeration, well dispersed and high aspect ratio of Silica at low loadings	Solution mixing
EP/SiO_2 4 wt.% [293]	42.3 (30.57%)	--	Optimal interaction of EP-SiO2 at 4 wt.%	Solution mixing
EP/SiO_2 13.4 vol.% [207]	--	3.85 (30%)	High modulus, well dispersion and no agglomeration of Silica	Sol-gel mixing
EP/SiO_2 20 wt.% [294]	--	3.97 (26.4%)	High stiffness of silica	Solution mixing
EP/SiO_2 20.2 wt.% [295]	--	3.85 (30%)	Well-dispersed silica	Solution mixing

MMT: montmorillonite; SMC: Silane-modified clay; SPU: Soft polyurethane; HPU: Hard polyurethane; EVA: Ethylene-vinyl acetate

Table 8: Mechanical properties of ceramic nano-particle reinforced metal matrix nanocomposites

Material	Hardness (GPa)	Tensile strength (MPa)	Yield strength (MPa)	Elongation (%)	Reasons	Fabricating methods
Al/SiC 3 wt.% [216]	0.55 (39.5%)	164.4 (29.3%)	145 (31%)	165.3 (-32.8%)	Homogenous distribution of SiC, effects of Orowan strengthening, grain size refinement (yield strength), mismatch of thermal expansion coefficients between Al and SiC (CTE). Porosities lead to a reduction of ductility. SiC hindered metal matrix dislocation that increasing hardness	Powder metallurgy (PM), ultrasound-assisted stirring and planetary agitation, hot compressing
Al/SiC 6.5 vol.% [219]	--	807 (26.5%)	610.8 (9.5%)	59 (-91.8%)	Homogenous dispersed SiC, grain size refinement, Orowan strengthening	Mechanical alloying, cryo-milling, HIP consolidation
Al/SiC 1.25 vol.% [222]	-- (69%)	-- (109%)	--	3.6 (-40%)	Homogenous distribution of SiC and CTE strengthening at low loading, residual stresses, high dislocation density and grain size reduction increased hardness, agglomeration and porosity at a high loading of SiC. Hard particles reduced ductility.	Mechanical alloying, ultra-sonication
Al/SiC 2 wt.% [228]	--	301 (12%)	156.3 (43.4%)	3.4 (26%)	Uniformly dispersed SiC, CTE, high dislocation density, restriction of dislocations	Mechanical alloying, ultra-sonication
Al/Al_2O_3 4 vol.% [217]	66.6 (109.5%)	245.5 (67%)	183.7 (138.6%)	12.8 (-51.7%)	Evenly distributed Al2O3 Orowan strengthening and grain size refinement effects at below 4 vol.% of loading	PM, wet mixing, cold isotropic pressing (CIP) and sintering
Al alloy/SiC 10 wt.% [227]	87.2 BHN (9%)	265 (12.3%)	257 (16.8%)	18.2 (-6.2%)	The composite density was reduced, SiC hindered alloy dislocations, uniform distribution of SiC and their high wettability due to Mg coating	Stir casting
Al alloy/SiC 10 wt.% [226]	78 BHN (28%)	188 (0.53%)	--	2.4 (-22.6%)	Insufficiently homogenous distribution of SiC due to improper stirring led to the low improvement of tensile strength, hard	PM, mechanical mixing

					SiC hindered dislocations that contributed to hardness improvement	
Al alloy/SiC 6 wt.% [296]	116 BHN (62%)	267 (29%)	--	3.6 (-41%)	SiC possessed advanced hardness, strong interface of Al alloy - SiC	Liquid metallurgy
Mg alloy/SiC 1.5 wt.% [224]	--	199.3 (90%)	71.7 (73%)	20 (135%)	Grain size refinement, strong bond of Mg/4Zn-SiC, SiC clusters, no reason for ductility improvement	MA, ultrasonic cavitation
Mg/SiC 3 vol.% [225]	0.58 (180%)	288 (21.5%)	--	6 (-40%)	Grain size refinement, dispersion hardening, strain hardening due to extrusion, dislocation hindering	PM, ball milling
Mg/SiC 1.84 wt.% [223]	0.42 (10%)	203 (18%)	157 (25.6%)	7.6 (31%)	Hard SiC led to a high constraint of matrix deformation that improved hardness, dislocation density, internal stresses formation due to thermal expansion mismatch, Orowan strengthening and the mismatch of elastic reinforcing phase - plastic matrix phase contributed to tensile properties increments, the activation of non-basal slip and SiC-Mg interfacial integrity led to ductility improvement	MA, pressing, microwave hot sintering
Mg/SiO_2 10 vol.% [297]	1.03 (75%)	251 (32%)	225 (60.7%)	4 (-69%)	Uniform distribution of SiO2, grain size refinement, Mg2Si, MgO formations during FSP	FSP
Al/TiC 10 wt.% [221]	44.17 HV5 (143.6%)	--	189 (136%)	5 (-83.3%)	Strong TiC particles, grain size refinement	In situ